A Thesis for the Degree of Ph.D. in Engineering

Physiological Characterization of Event-Related Desynchronization in Human Electroencephalogram

May 2015

Graduate School of Science and Technology

Keio University

Mitsuaki Takemi

Contents

1. General Introduction 1

1.1 Corticospinal System in Voluntary Movements 1

1.2 Technique to Assess Corticospinal Excitability 5

1.2.1 Transcranial Magnetic Stimulation 5

1.2.2 F-wave and H-reflex 7

1.3 Effects of Motor Imagery on the Corticospinal Excitability 9

1.4 Event-Related Desynchronization in Electroencephalogram 12

1.5 Brain-Computer Interface for Neurorehabilitation 17

1.6 Purpose of The Dissertation 19

2. Event-Related Desynchronization Reflects Downregulation of Intracortical Inhibition in Human Primary Motor Cortex 21

2.1 Introduction 21

2.2 Materials and Methods 23

2.2.1 Participants 23

2.2.2 Data Acquisition 24

2.2.3 Experimental Protocol 25

2.2.4 Electroencephalogram Analysis 29

2.2.5 Motor Evoked Potential Analysis 31

2.2.6 Statistical Tests 32

2.3 Results 32

2.3.1 Spectral Power of Electroencephalogram 32

2.3.2 Changes of the Intracortical Excitability 35

2.3.3 Effects of Task Compliance on Intracortical Excitability 41

2.4 Discussion 43

2.4.1 Relationship between Sensorimotor Event-Related Desynchronization and Intracortical Excitability 43

2.4.2 Frequency Components of Event-Related Desynchronization Representing Cortical Excitability 46

2.4.3 Muscle Dependency and Motor Imagery Task 47

3. Event-Related Desynchronization Represents the Excitability of Human Spinal Motoneurons 49
3.1 Introduction 49
3.2 Materials and Methods 50
3.2.1 Participants 50
3.2.2 Data Acquisition 51
3.2.3 Experimental Protocol 52
3.2.4 F-wave Analysis 54
3.2.5 Electroencephalogram Analysis 55
3.2.6 Statistical Tests 56
3.3 Results 57
3.3.1 F-wave Measurements 57
3.3.2 Spectral Power of Electroencephalogram 62
3.3.3 Effects of Task Compliance on the Spinal Excitability 65
3.4 Discussion 67
3.4.1 Relationship between Sensorimotor Event-Related Desynchronization and the Spinal Excitability 67
3.4.2 Association of the Topography of Event-Related Desynchronization with Spinal Excitability 69
3.4.3 Comparison of F-wave and H-reflex Responses 70
3.4.4 Physiological Interpretation of Event-Related Desynchronization during Motor Imagery 71
Conclusions 75
Acknowledgement 79
References 81
Bibliography 89

List of Figures

Figure 1-1. A brain circuit for voluntary actions 2
Figure 1-2. Cortical origins of the corticospinal tract 3
Figure 1-3. Divergent corticomotoneuronal connections that innervate different arm muscles 4
Figure 1-4. Principles of TMS.....5
Figure 1-5. MEP size changes in response to the paired pulse TMS paradigm 7
Figure 1-6. Pathways involved in the production of the F-wave and H-reflex 10
Figure 1-7. International 10-20 System for EEG electrode placement 13
Figure 1-8. Thalamo-cortical connections involved in the generation of brain rhythmic activity (ERD and ERS) 15
Figure 1-9. Diagram of the relationship between cortical activation, excitability level of neurons, and availability of neurons for synchronization 16

Figure 2-1. Experimental setup and paradigm 28
Figure 2-2. Method for ERD analysis 30
Figure 2-3. ERD time-frequency map in the screening session.....34
Figure 2-4. ERD topographies and MEP traces in one representative participant (Participant 1A) 37
Figure 2-5. MEP amplitude, SICI, and ICF in the resting condition and during wrist motor imagery at ERD 5% and 15% 38
Figure 2-6. Relationship between the ERD frequency band and SICI during motor imagery of wrist flexion and wrist extension 40
Figure 2-7. Correlation between SICI, percentage of task success, and duration of the motor imagery before stimulation 42
Figure 2-8. An example of an ERD time course during the motor imagery task.....45

Figure 3-1. Experimental setup and paradigm 54
Figure 3-2. M- and F-wave traces and ERD topographies in one representative participant (Participant 1A) 58
Figure 3-3. F-wave measurements in the resting condition and during hand motor imagery at ERD 5% and 15%.....59

Figure 3-4. Relationship between ERD frequency band and F-wave persistence 61
Figure 3-5. ERD topographies on the apparent and non F-wave trials during hand motor imagery 64
Figure 3-6. Correlation between F-wave persistence, (a) percentage of task success, and (b) duration of motor imagery before nerve stimulation 66
Figure 3-7. Schematic diagram of the neural activity changes related to the generation of ERD during motor imagery 74

List of Tables

Table 2-1. Frequency band and bipolar channel displaying the largest ERD during right wrist motor imagery in the screening session 35
Table 2-2. TMS measurements in the resting condition, and wrist motor imagery at ERD 5% and 15% 39

Table 3-1. F-wave measurements in the resting condition, and during right hand motor imagery at ERD 5% and ERD 15% 60
Table 3-2. Frequency band and bipolar channel displaying the largest ERD during right thumb abduction in the screening session 62
Table 3-3. EEG channels with significant difference in ERD values between apparent and non F-wave trials 65

Abbreviations

ANOVA	analysis of variance
APB	abductor pollicis brevis
BCI	brain-computer interface
BOLD	blood oxygen level dependent
CMAP	compound muscle action potential
ECR	extensor carpi radialis
EEG	electroencephalogram
EMG	electromyogram
ERD	event-related desynchronization
ERS	event-related synchronization
FCR	flexor carpi radialis
fMRI	functional magnetic resonance imaging
GABA	γ-aminobutyric acid
ICF	intracortical facilitation
ISI	interstimulus interval
ITR	inhibitory thalamic reticular
M1	primary motor cortex
MEP	motor evoked potential
PMd	dorsal premotor area
PMv	ventral premotor area
S1	primary somatosensory cortex
SICI	short interval intracortical inhibition
SMA	supplementary motor area
TCR	thalamocortical relay
TMS	transcranial magnetic stimulation

Chapter 1

General Introduction

1.1 Corticospinal System in Voluntary Movements

Human brains contain several distinct cortical motor circuits that contribute to voluntary movements. These circuits converge to the primary motor cortex (M1), which executes motor commands by transmitting them to the spinal cord and muscles. Thus, M1 is considered to be a 'final common path determiner of movement' (Goldring and Ratcheson, 1972). One key input reaches to M1 from the ventral premotor area (PMv) and dorsal premotor area (PMd), which in turn receive input from the parietal association cortex (Fig. 1-1). This parietal-premotor circuit guides object-oriented voluntary actions, such as grasping, using current sensory input that is served from the primary somatosensory cortex (S1). However, recent studies suggest that the parietal-premotor circuit contributes to not only object-oriented actions but also self-paced actions (Gold and Shadlen, 2007; Shadlen and Newsome, 2001).

To produce movement, motor commands originated from cortical motor circuits must reach the spinal motoneurons. The corticospinal system is therefore involved in the control of all aspects of body movement. In humans, the corticospinal tract consists of approximately one million axons, of which 30% to 40% originate from neurons in the M1. M1 is the only area of motor cortex that monosynaptically connects with spinal motoneurons. These monosynaptically projecting cortical neurons are called corticomotoneurons. The rest of the axons have their origins mainly in the parietal association cortex and in the premotor cortex

(Fig. 1-2), which consists of several functionally distinct areas, such as PMv, PMd, and the supplementary motor area (SMA). The premotor cortex sends fibers to interneurons in the intermediate zone of the spinal cord (Dum and Strick, 1991). The parietal association cortex sends fibers to the dorsal horn that contains the sensory neurons of the spinal cord. All of corticospinal axons from these various areas descend through the subcortical white matter, internal capsule, and the pyramidal decussation, and terminate in the spinal cord of the opposite side.

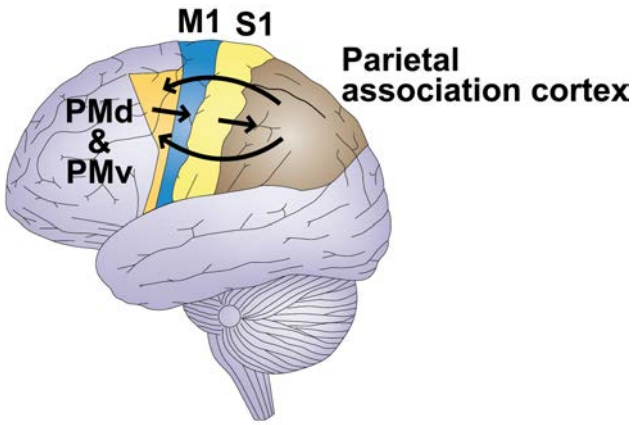

Figure 1-1. A brain circuit for voluntary actions

Information from the S1 is relayed to the parietal association cortex, and from there to the PMv and PMd, which project in turn to the M1. This parietal–premotor circuit not only guides object-oriented actions, such as grasping, using current sensory input, but also contributes to some aspects of self-paced actions (Modified from Haggard, 2008).

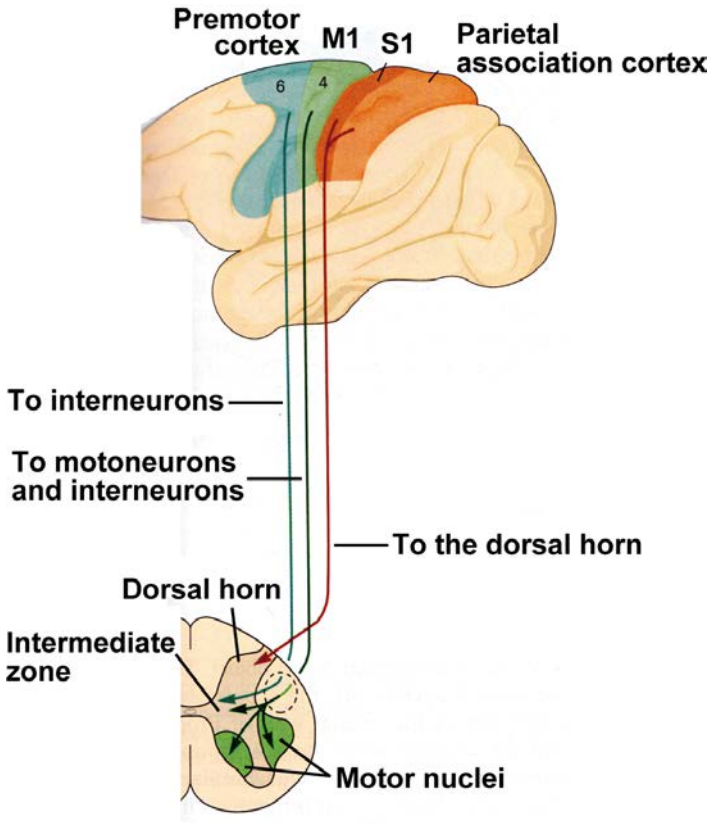

Figure 1-2. Cortical origins of the corticospinal tract

Neurons that modulate the activity in the contralateral arm and hand muscles originate in the M1, S1, parietal association cortex, and many subdivisions of the premotor cortex, such as the PMv, PMd, and SMA (Modified from Rizzolatti and Strick, 2013).

The terminal of a single corticomotoneuronal axon often branches and terminates on spinal motoneurons for several different agonist muscles. A single corticomotoneuron can also influence the contractile activity of still more muscles through synapses on spinal interneurons (Fig. 1-3). This termination pattern is functionally organized to produce coordinated patterns of activity in a muscle field of agonist and antagonist muscles. Most frequently, a single corticomotoneuron excites the spinal motoneurons for several agonist muscles and indirectly suppresses the activity of some antagonist muscles through local inhibitory interneurons. Comparing corticomotoneurons projecting to wrist flexor and

extensor muscles in primates, the extensor corticomotoneurons have a larger muscle field than the flexor corticomotoneurons (Fetz and Cheney, 1980; Kasser and Cheney, 1985). The flexor corticomotoneurons have the ability to inhibit as well as to facilitate their target spinal motoneurons, whereas the extensor corticomotoneurons appear only to have descending facilitatory control (Cheney *et al.*, 1985). This anatomical finding suggests that an ability to modulate the corticospinal excitability of flexor muscles and extensor muscles induced by preparation or imagery of agonist muscle contraction might not be equivalent.

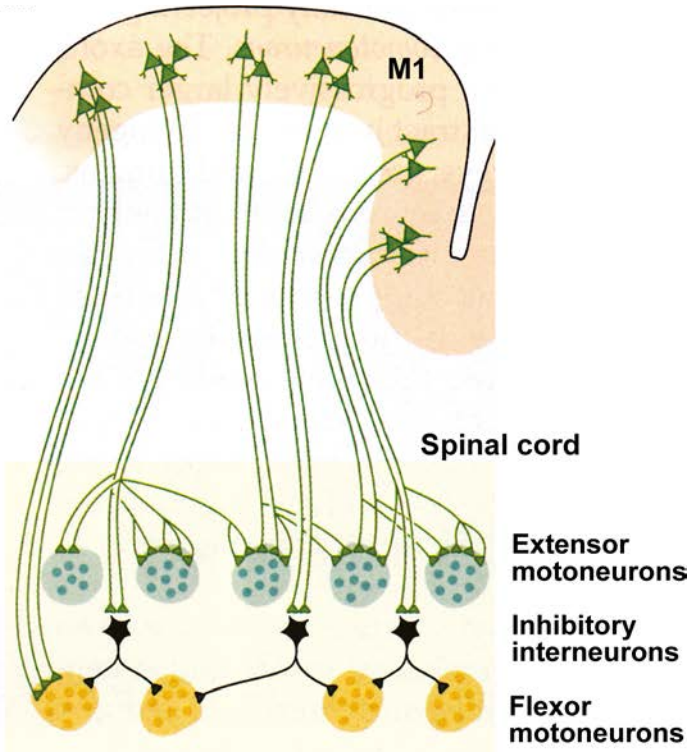

Figure 1-3. Divergent corticomotoneuronal connections that innervate different arm muscles

Corticomotoneurons in the M1 project their fibers monosynaptically to the spinal motoneurons. Different colonies of corticomotoneurons in the M1 terminate on different combinations of spinal interneurons and motoneurons, thus activating different combinations of flexor and extensor muscles (Modified from Kalaska and Rizzolatti, 2013).

1.2 Technique to Assess Corticospinal Excitability

1.2.1 Transcranial Magnetic Stimulation

Transcranial magnetic stimulation (TMS) is a noninvasive brain stimulation technique, which uses a rapidly changing magnetic field to elicit electric currents that excites cortical neurons running parallel to the cortical surface via electromagnetic induction (Fig. 1-4). TMS causes to fire layer V pyramidal neurons indirectly via interneurons (I-waves) that originate in cortical layer II and III (Di Lazzaro *et al*., 2012). The stimulus-induced muscle activity, called motor evoked potential (MEP), is recorded by surface electromyogram (EMG). Depends on a number of stimulus pulses and its intensity, TMS enables to assess various phenomena related to the cortical or corticospinal excitability.

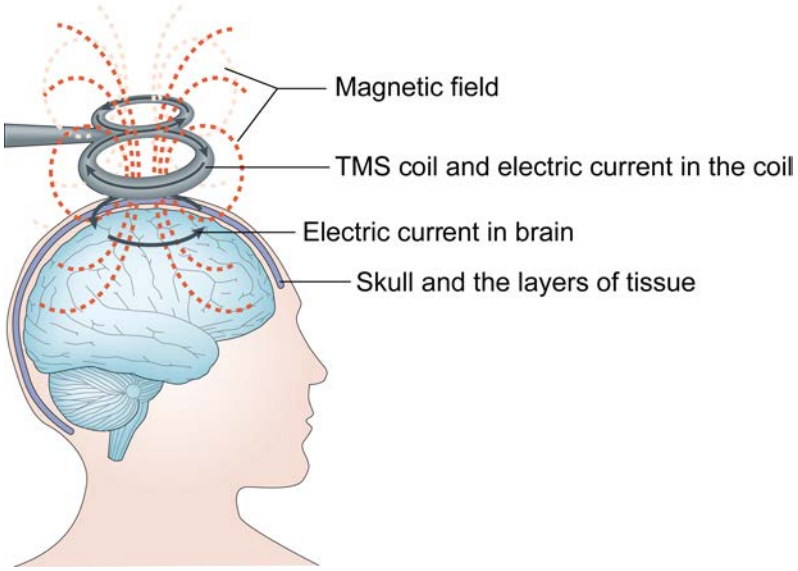

Figure 1-4. Principles of TMS

A brief strong electric current travels through the coil held over the scalp, setting up a perpendicularly directed magnetic field. A rapidly changing magnetic field is passed through the skull and layers of tissue, and produces an electric current in the cortex running parallel to the cortical surface (Modified from Ridding and Rothwell, 2007).

Single pulse TMS provides information about corticospinal excitability by measuring variables such as motor threshold (the threshold stimulation intensity at which an MEP can be elicited) and MEP amplitudes (Day *et al*., 1989). In this technique, TMS coil is generally held over the M1 in the optimal position for eliciting a response in the muscle of interest. Additionally, the recruitment curve (the slope of the increase in MEP amplitude with increasing stimulation intensity) and the motor map area (size of the scalp area over which an MEP can be elicited) convey information of corticospinal excitability (Cohen *et al*., 1991).

Paired pulse TMS is delivered through one or two separate magnetic coils at varying inter-stimulus intervals (ISIs) to elicit measurable inhibition or facilitation (Fig. 1-5). For paired pulses delivered to the same hemisphere at short ISIs (1–4 ms), the MEP produced by a suprathreshold test stimulus preceded by a subthreshold conditioning stimulus is smaller than that produced by an test stimulus alone (Kujirai *et al*., 1993). This phenomenon is referred to as short interval intracortical inhibition (SICI). SICI is quantified as the MEP amplitude produced by the conditioned test stimulus expressed as a percentage of that produced by the test stimulus alone. Pharmacological study provided more detailed information about the mechanisms of SICI. γ-aminobutyric acid $(GABA)_A$ agonists enhance SICI (Ziemann *et al*., 1996). The magnitude of SICI is considered to represents the activity of $GABA_A$ interneurons in M1.

Paired pulses delivered to the same hemisphere at ISIs of 8–20 ms, using a subthreshold conditioning stimulus to influence the response to a subsequent suprathreshold test stimulus, induces larger MEP compared to the MEP produced by the test stimulus alone (Kujirai *et al*., 1993). This phenomenon is termed intracortical facilitation (ICF). Since Dextromethorphan, which is *N*-methyl-D-aspartate antagonists, abolishes ICF (Ziemann *et al*., 1998), the

magnitude of ICF appears to reflect the activity of excitatory glutamatergic interneurons within M1 and *N*-methyl-D-aspartate receptors.

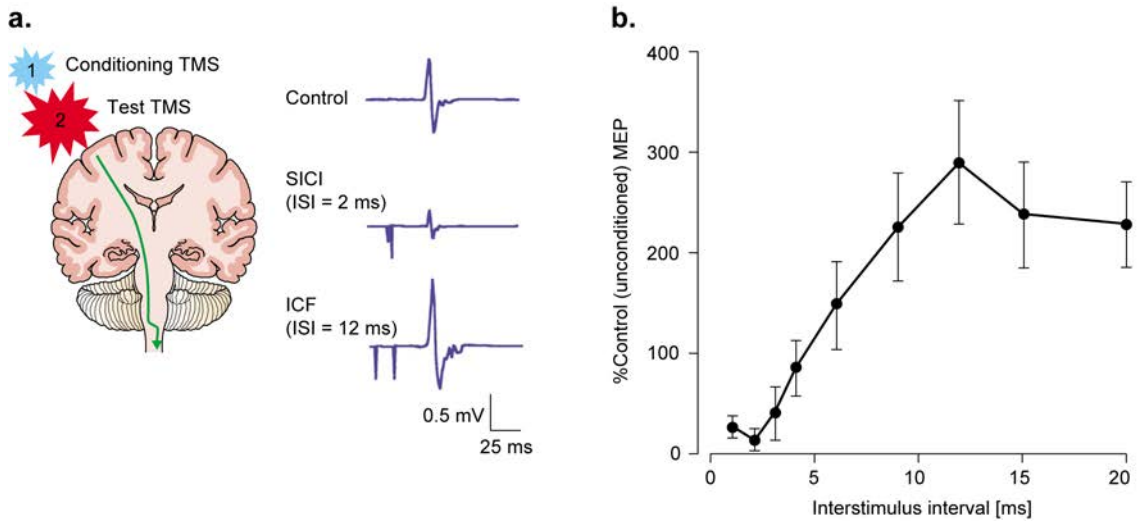

Figure 1-5. MEP size changes in response to the paired pulse TMS paradigm

(a) Illustrated MEP traces were recorded from the first dorsal interosseus muscle. (b) The MEP sizes are expressed as a percentage of the control (unconditioned) MEPs, and plotted against the ISI. The conditioning stimulus inhibits the test MEP at short ISIs (1–4 ms) but facilitates it at longer intervals (8–20 ms) (Modified from Kobayashi and Pascual-Leone, 2003).

1.2.2 F-wave and H-reflex

F-wave and H-reflex are methods for testing the excitability of human spinal motoneurons induced by the peripheral nerve stimulation. Both responses can be recorded using surface EMG, but the technique to elicit response and its physiological mechanism are different.

The F-wave reflects backfiring of a small number of motoneurons, which are reactivated by antidromic impulses following supramaximal stimulation of a peripheral nerve (Fig. 1-6a). When applying to the supramaximal stimulation, large orthodromically evoked

compound muscle action potential (CMAP), called the maximal M-wave, is firstly observed, and then small antidromically evoked CMAP (F-wave) is observed. The latency of a F-wave therefore includes the time required for the action potential to travel antidromically from the site of electrical stimulation to the anterior horn cells (spinal motoneurons) and the time to travel orthodromically from the anterior horn cells to the muscle. Because F-waves are small (often less than 0.5 mV) and varied in size and shape, large number of responses is collected for averaging its amplitude and calculating the percentage of stimuli evoking a response (Lin and Floeter, 2004).

Typical F-wave measurement in excitability experiments is mean amplitude and persistence. Mean F-wave amplitude is obtained by averaging the unrectified amplitude of each F-wave measured either ignoring instances when no F-wave is seen or recording them as zero. An increase in mean F-wave amplitude that ignores trials where no F-waves are recorded would indicate a shift in motor units recruited from smaller ones to larger ones. If trials where no responses are included, this measure would be influenced by the excitability of total spinal motoneurons. F-wave persistence is the percentage of times an apparent F-wave is recorded relative to the number of stimuli presented. This measure probably best reflects an increase in motoneuron excitability. F-wave latency, the most sensitive measures of diffuse nerve disorder, is unlikely to be influenced by cortical activity (Rivner 2008).

H-reflex is evoked by the submaximal stimulation and reflects the response of the motoneurons to a volley from Ia afferent fibers (Fig 1-6b). Comparison of H-reflex size to the maximal M-wave enables to estimate the motoneurons involved in the H-reflex. Similar to the descending input during voluntary contractions, the synaptic Ia input will recruit motoneurons in an orderly fashion from smallest to largest according to the Henneman size principle (McNeil *et al*., 2013), though F-wave occurs preferentially in large motoneurons

because the antidromic volley collides with the H-reflex impulse in small motoneurons. The sensitivity of the H-reflex to the changes in motoneuronal excitability is better than that of the F-wave (Hultborn and Nielsen, 1995). However, the H-reflex size is altered by spinal motoneuron excitability as well as mechanisms acting on the afferent volley (e.g., presynaptic inhibition), whereas occurrence of the F-wave solely depends on the excitability of spinal motoneurons (Pierrot-Deseilligny and Burke, 2005).

1.3 Effects of Motor Imagery on the Corticospinal Excitability

Motor imagery, defined as internal rehearsal of a movement without any overt physical movement (Decety, 1996), has been demonstrated beneficial in sports training (Lotze and Halsband, 2006) and motor rehabilitation in patients with movement disorders (Jackson *et al*., 2001; Riccio *et al*., 2010). The neuronal representations of motor imagery have been studied intensively for years using brain imaging techniques, such as functional magnetic resonance imaging (fMRI), electroencephalogram (EEG), and positron emission tomography (Dechent *et al*., 2004; Gao *et al*., 2011; Halder *et al*., 2011; Naito *et al*., 2002; Neuper *et al*., 2005; Porro *et al*., 1996; Yuan *et al*., 2010). These studies demonstrated that the brain activation pattern was similar to the brain regions activated during actual movement, such as M1, S1, SMA, PMv, PMd, and inferior parietal lobule that is a part of parietal association cortex, when a participant follows the instruction ‘imagine yourself performing a specific action’ (termed kinesthetic motor imagery). If the instruction is ‘imagine observing yourself performing an action as in a picture’ (termed visual motor imagery), the motor system is weakly activated. Thus, kinesthetic motor imagery corresponds to a subliminal activation of the motor system, with similar mechanism underlying movement execution.

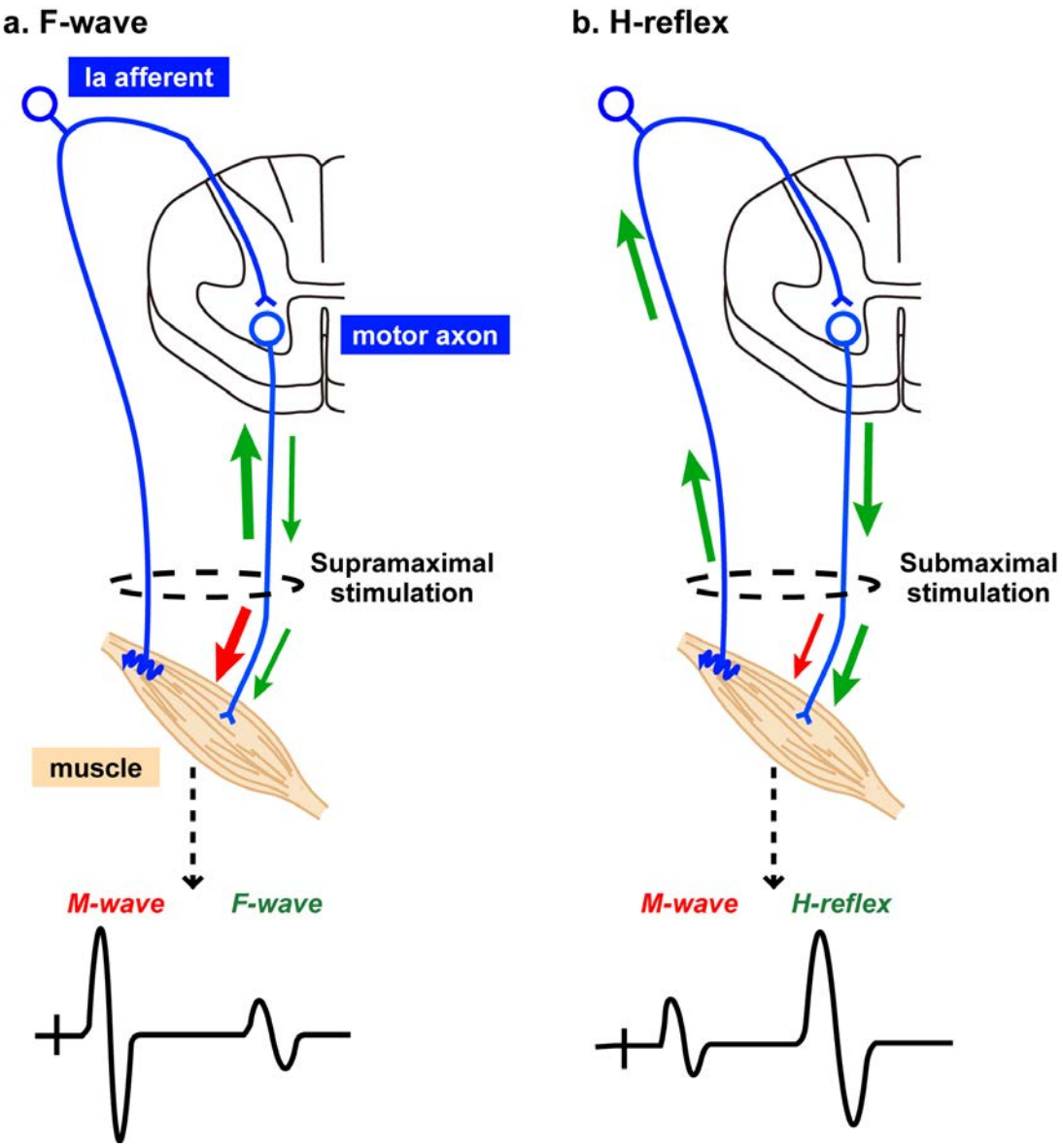

Figure 1-6. Pathways involved in the production of the F-wave and H-reflex

(a) A small number of motoneurons discharge to produce F-waves after antidromic impulses reach their soma. The orthodromic response (M-wave) precedes the antidromic response of the spinal motoneurons (F-wave). F-wave occurs preferentially in large motoneurons because the antidromic volley collides with the H-reflex impulse in small motoneurons. (b) Submaximal stimulus evokes a single afferent volley that recruits motoneurons for the H-reflex according to the size principle.

fMRI and positron emission tomography measure hemodynamic cortical activity but not necessarily electric cortical excitability. EEG reflects electric neural activity but is inferior in spatial resolution. Therefore, excitability in a specific cerebral area is generally examined by single and paired pulse TMS. It is well known that MEPs following single pulse TMS to the M1 are enhanced in the muscles during imagination of their movements (Abbruzzese *et al*., 1996; Facchini *et al*., 2002; Hashimoto and Rothwell, 1999; Kasai *et al*., 1997; Kier *et al*., 1997; Rossini *et al*., 1999; Sohn *et al*., 2003; Yahagi and Kasai, 1998). Stinear *et al*. (2006) demonstrated that kinesthetic, but not visual, motor imagery increased corticospinal excitability. Paired pulse TMS paradigm clarified SICI was significantly reduced during motor imagery but not ICF (Patuzzo *et al*., 2003). All of them show that increase in the M1 excitability during motor imagery is evident.

Both H-reflex and F-wave techniques, in combination with TMS over M1, have been used to explore the changes in supraspinal and spinal excitabilities during motor imagery. Some researchers have found no effect of motor imagery on H-reflex (Abbruzzese *et al*., 1996; Hashimoto and Rothwell, 1999; Kasai *et al*., 1997; Patuzzo *et al*., 2003), whereas others have found a facilitatory effect in half of their subjects, resulting in a statistically significant difference (Kiers *et al*., 1997). Another study also found significant increase in H-reflex amplitude during motor imagery, and they argued that it was yielded in subthreshold activation of spinal motoneurons elicited by the increased M1 excitability accompanying motor imagery (Gandevia *et al*., 1997). Rossini *et al*. (1999) reported specific facilitation of the F-waves recorded from intrinsic hand muscles during motor imagery. On the other hand, there was no change in F-waves in some motor imagery studies, also recorded from intrinsic hand muscles (Facchini *et al*., 2002; Sohn *et al*., 2003; Stinear *et al*., 2006). Thus, in contrast to the effect of motor imagery on the M1 excitability, whether motor

imagery alters spinal excitability is still under debate.

1.4 Event-Related Desynchronization in Electroencephalogram

EEG is one of the oldest and most widely used methods for the investigation of the electric activity of the brain. The scalp EEG, recorded by a single electrode on the scalp, is a spatiotemporally smoothed version of the local field potential, integrated over an area of 10 cm^2 or more (Buzsáki *et al*., 2012). In standard practice, the electrode position for EEG recording is defined by the International 10-20 System (Fig. 1-7). This relies on taking measurements between certain fixed points on the head. The electrodes are then placed at points that are 10% and 20% of these distances. Each electrode site is labeled with letter and number. Of note, EEG channel of C3 and C4 generally correspond to the hand area of S1 and M1 and partially overlap with the premotor cortex.

Studies of oscillatory EEG signals in the sensorimotor and premotor cortices provide an implication of how the information processing related to voluntary movements in multiple motor areas is accomplished. Actual movement as well as motor imagery and movement preparation produces an event-related desynchronization (ERD), which is a decrease in EEG amplitude, over the sensorimotor area in the frequency range of alpha (7–13 Hz) and beta (14–26 Hz) bands (Gerloff *et al*., 2006; Neuper *et al*., 2005; Pfurtscheller and Lopes da Silva, 1999). ERD is the most prominent over the contralateral sensorimotor area during motor preparation and extends bilaterally with movement initiation. ERD during hand motor imagery is very similar to the pre-movement ERD, i.e., it is mainly observed over the contralateral sensorimotor area (Neuper and Pfurtscheller, 1999). A localized sensorimotor ERD is interpreted as an electrophysiological correlate of an activated cortical area, and a localized event-related synchronization (ERS), which is an amplitude increase, is typically

viewed as a correlate of a deactivated cortical area and may represent idling or inhibitory cortical activity (Pfurtscheller *et al*., 1996).

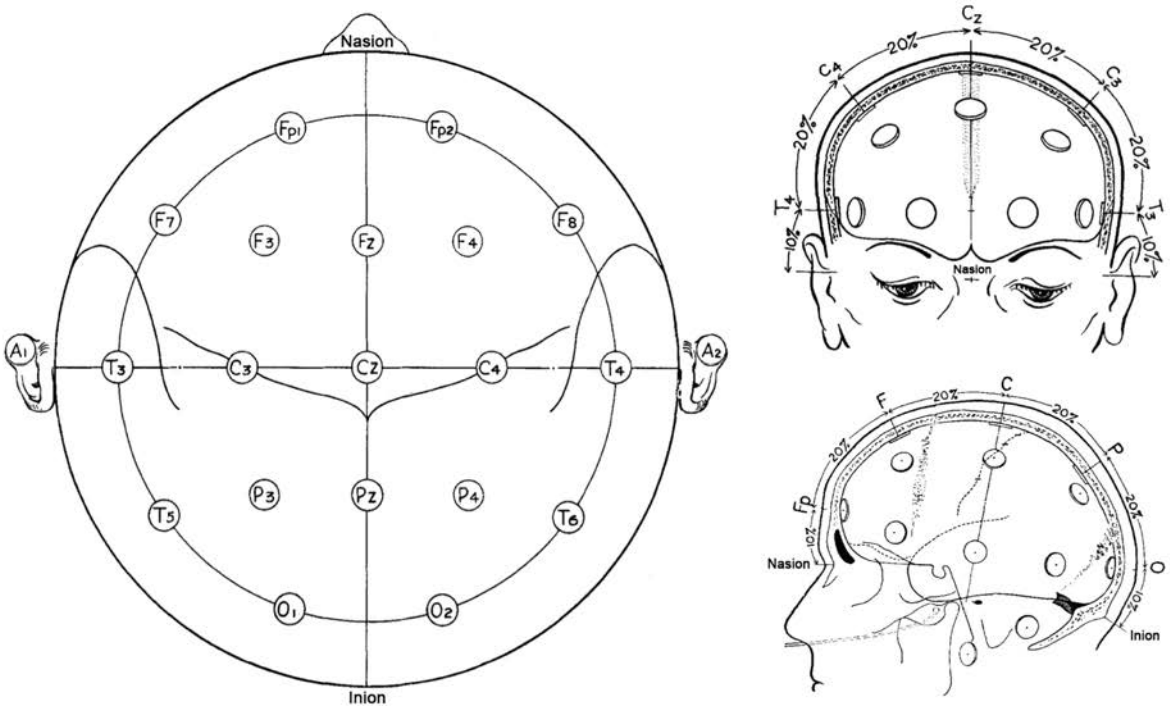

Figure 1-7. International 10-20 System for EEG electrode placement

A system of EEG electrode placement on the scalp in which the adjacent electrodes are placed in a line at either 10% or 20% of the total distance on the skull between the nasion and inion in the sagittal plane and between the right and left preauricular points in the coronal plane. Capital letters “Fp”, “F”, “T”, “C”, “P”, and “O” correspond to the prefrontal, frontal, temporal, central, parietal, and occipital cortices, respectively. The small letter “z” refers to an electrode on the midline. Even numbers refer to electrodes on the right hemisphere, and odd numbers refer to those on the left hemisphere. The letter ‘A’ represents the earlobes (Modified from Jasper, 1958).

Several studies attempted to investigate the mechanism of changes in brain rhythmic activity. In 1980s, it had been proposed that brain oscillations in neural populations might be determined by neuronal pacemakers as in the heart. However, Steriade and Llinás (1988) revealed the thalamo-cortical relay (TCR) nucleus could not generate spindle oscillations after disconnection from the inhibitory thalamic reticular (ITR) nucleus. This finding suggested the interplay between the TCR neurons and the ITR neurons plays an important role in the control of the cortical dynamics of brain oscillations (Fig. 1-8). Further, Pfurtscheller and Lopes da Silva (1999) depicted the generation model of ERD. This model illustrated ERD results from changes in the functional connectivity within the thalamo-cortical feedback loop. The changes can be due to a variety of factors. In particular, they may depend on modulating influences arising from cholinergic input from the brain stem afferents (Suffczynski *et al*., 1999).

Recently, Pfurtscheller (2006) proposed the Cortical Activation Model (Fig. 1-9), which demonstrated the relationship between cortical activation and the amplitude of EEG oscillations. He argued that the cortical activation results in phasic changes in synchrony of cell population in the sensorimotor area due to externally or internally paced events. This model attempted to demonstrate whether an internally or externally paced event explains an ERD or ERS in a specific frequency band. The amplitude of network-specific oscillations depends on, in addition to other factors, the number of neurons available for synchronization and the excitability level of neurons.

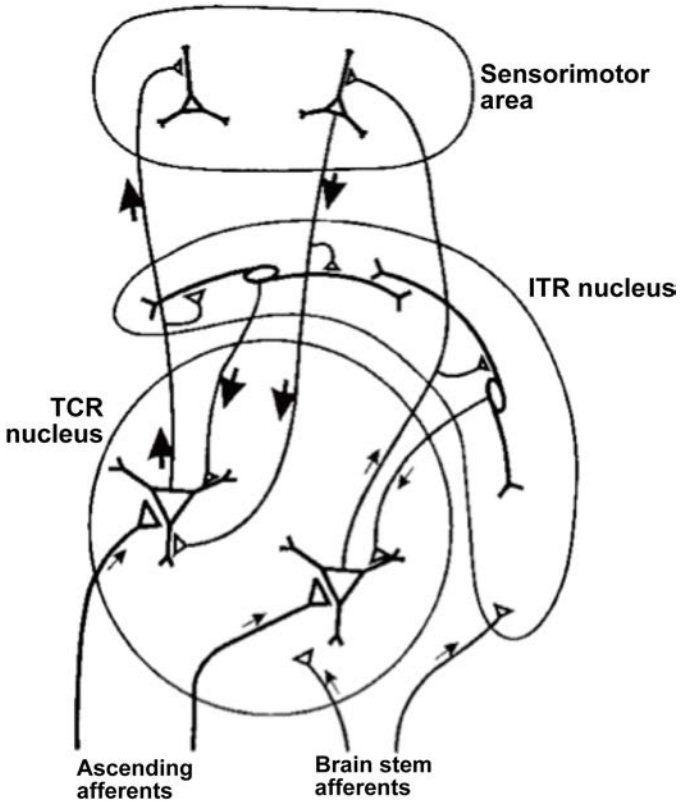

Figure 1-8. Thalamo-cortical connections involved in the generation of brain rhythmic activity (ERD and ERS)

Each TCR neuron receives inputs from the ascending afferents and projects upon a localized region of the sensorimotor area. The TCR neurons also send excitatory inputs to the inhibitory ITR neurons. The ITR neurons are connected to each other and send back fibers to the TCR neurons. The connection of the excitatory TCR neurons and inhibitory ITR neurons creates a negative feedback loop and contributes to the generation of intrinsic cortical oscillations. Both TCR and ITR neurons receive cholinergic modulatory input from the brain stem afferents (Modified from Pfurtscheller and Lopes da Silva, 1999).

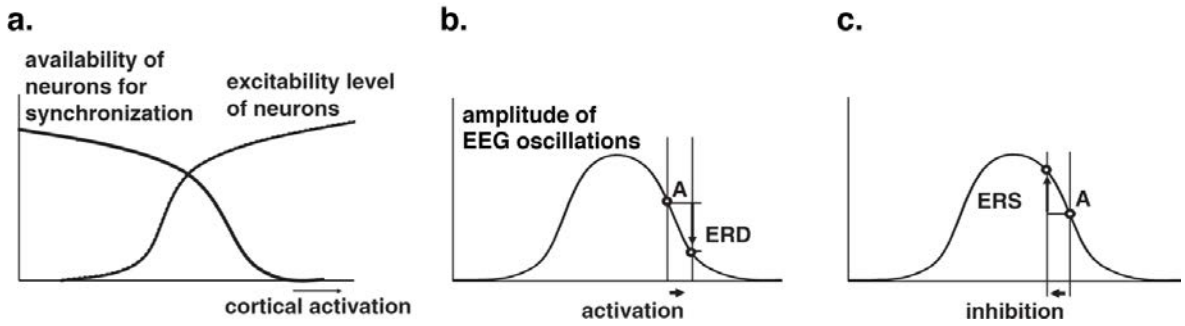

Figure 1-9. Diagram of the relationship between cortical activation, excitability level of neurons, and availability of neurons for synchronization

(a) The relationship between cortical activation (horizontal axis) and amplitude of EEG oscillations in a specific frequency band. The right vertical axis represents the excitability level of neurons, and the left vertical axis represents the availability of neurons for synchronization. (b) ERD or ERS depends on the baseline level of the cortical activation at the time-point of an externally or internally paced event. At a certain baseline level of the cortical activation (point A), an increase in the cortical activation results in an ERD. (c) A decrease in the cortical activation (inhibition) induces an ERS (Modified from Pfurtscheller, 2006).

Motor imagery-induced ERD and the blood oxygen level dependent (BOLD) signal by fMRI co-localized at the sensorimotor area, and the magnitudes of ERD and BOLD co-varied (Formaggio *et al*., 2010; Yuan *et al*., 2010). These results supported the Cortical Activation Model in which ERD during motor imagery represents increase in the sensorimotor cortical activation. Simultaneous TMS-EEG technique provided the evidence of a concurrent increase of MEPs induced by single pulse TMS over the M1 and sensorimotor ERD at 11–13 Hz during motor imagery (Hummel *et al*., 2002). More recently, a positive correlation between the alpha or beta band ERD and the MEP amplitude was shown (Mäki and Ilmoniemi, 2010; Sauseng *et al*., 2009; Shultz *et al*., 2013). Nevertheless, it

remains unclear whether ERD during motor imagery recorded over the sensorimotor area actually represents either or both the excitability of M1 and spinal motoneurons, because MEP induced by the single pulse TMS reflects the corticospinal excitability but not the independent excitabilities of the M1 and spinal motoneurons. Concurrent use of EEG with paired pulse TMS enables to identify what parts of the intracortical circuits involved in motor output change their activity during motor imagery accompanied by ERD.

Addition to the sensorimotor area, ERD was observed over the SMA and the posterior association cortex during voluntary hand movement (Babiloni *et al*., 1999). It has been suggested that ERD over the SMA and the posterior association cortex reflects the regional cortical activity (Chen *et al*., 2010; Ritter *et al*., 2009). Information from the parietal association cortex is relayed to PMv and PMd and thence to the M1, which executes motor commands by transmitting them to the spinal motoneurons for the initiation of voluntary movements. SMA has efferent fibers to the spinal interneurons. Thus, the activity in these higher motor cortices might influence on the excitability of spinal motoneurons. However, there is no empirical evidence of the relationship between ERD over the higher motor cortices and the excitability of spinal motoneurons.

1.5 Brain-Computer Interface for Neurorehabilitation

Recent advance in neurotechnology has led to an increased interest in the brain-computer interface (BCI) that translates brain activity into control signals of computer or machines, e.g., neuroprosthetics or robotic devices (Daly and Wolpaw, 2008), as a tool for rehabilitation in stroke patients with severe hemiplegia. This type of BCI often exploits ERD in scalp EEG recorded over the sensorimotor area, which is observed when patients attempt to move the paretic hand, and provides immediate sensory and/or visual feedback contingent

upon their ipsilesional ERD. Stroke rehabilitation using the ERD-based BCI demonstrated significant recovery of motor function in the paretic limb (Ang *et al*., 2011, 2014; Buch *et al*., 2008; Mukaino *et al*., 2014; Ono *et al*., 2014; Ramos-Murguialday *et al*., 2013; Shindo *et al*., 2011; Várkuti *et al*., 2012; Young *et al*., 2014). Thus, the ERD-based BCI is believed to somehow affect the neural plasticity that facilitates motor recovery. One possible mechanism is that the visual and sensory feedback of whether the ERD has occurred serves as a reward in the framework of reinforcement learning, and it enables to control the brain oscillatory activity that is translated into a reaching and grasping movement of the paretic limb (Ramos-Murguialday *et al*., 2013). Other hypothesized mechanism behind such plasticity involves simultaneous activation of inputs and outputs to the motor cortices by immediate sensory feedback contingent upon their ipsilesional ERD. This would trigger Hebbian-like plasticity and strengthen the ipsilesional sensorimotor loop (Soekadar *et al*., 2014).

The above-mentioned mechanisms that lead to the motor recovery are built on the idea that ERD reflects neural excitability. However, there is no empirical evidence of the relationship between the ERD during motor imagery and the excitability of corticospinal system, which is involved in the control of all aspects of limb movement. In the area of rehabilitation engineering, clarifying a relationship between EEG features (such as ERD) and the actual neural activity is an urgent issue for enhancing the efficacy of motor recovery by the BCI. Thus, the goal of this dissertation was to empirically reveal an association of the ERD during motor imagery with the excitabilities of the M1 and spinal motoneurons. This provides fundamental knowledge for establishing the technical principle of BCI rehabilitation.

1.6 Purpose of The Dissertation

The purpose of this dissertation is to investigate whether ERD in scalp EEG is a proper biomarker representing the excitability of the corticospinal system, which is involved in the control of all aspects of body movement. To achieve this goal, the research presented in this dissertation consists of two electrophysiological experiments.

In the first study (presented in Chapter 2), the association of sensorimotor EEG changes reflected by an ERD with the M1 excitability during kinesthetic motor imagery of the agonist muscle contraction was determined using single and paired pulse TMS. From the outcomes of SICI and ICF, I examined what parts of the intracortical circuits involved in motor output change their activity in conjunction with ERD during motor imagery. A relationship of the M1 excitability with the ERD magnitude during motor imagery of wrist flexion and extension was also compared, because the anatomical characteristics of the flexor corticomotoneurons in the M1 were not equivalent to the extensor corticomotoneurons (Cheney *et al*., 1985).

The second study (presented in Chapter 3) tested the relationship between ERD magnitude during kinesthetic motor imagery of the agonist muscle contraction and the excitability of spinal motoneurons, since the leaked cortical volley elicited by motor imagery may facilitate spinal motoneurons without overt muscle contractions. I used F-wave as a measure of spinal motoneuronal excitability in order to eliminate the effect of mechanisms acting on the afferent fibers from the present result. In addition, the difference in the ERD topography during motor imagery between the conditions of higher and lower spinal excitability were compared because of the anatomical finding by Dum and Strick (1991). It implied that the activity of both the M1 and higher motor cortices might influence spinal excitability.

Taken together, the research presented in this dissertation provides an evidence of the physiological characteristics of ERD during motor imagery and fundamental knowledge for establishing the technical principle of BCI rehabilitation. The ultimate goal of the studies is to open up new possibilities for the use of EEG-guided BCI that contributes to the treatment of various types of diseases, such as stroke and spinal cord injury.

Chapter 2

Event-Related Desynchronization Reflects Downregulation of Intracortical Inhibition in Human Primary Motor Cortex

2.1 Introduction

There is increasing interest in the use of BCI that translate electric, magnetic, or metabolic brain activity into control signals of computers or machines as a tool for rehabilitation of upper limb motor functions in severe hemiplegic stroke patients (Ang *et al*., 2011, 2014; Buch *et al*., 2008; Mukaino *et al*., 2014; Ono *et al*., 2014; Ramos-Murguialday *et al*., 2013; Shindo *et al*., 2011; Várkuti *et al*., 2012; Young *et al*., 2014). This type of BCI often exploits alpha and beta ERD in scalp EEG recorded over the sensorimotor area, which is observed when patients attempt to move paretic hand.

The generation mechanism of ERD was modeled by the phasic changes in the synchrony of cell populations (Pfurtscheller, 2006). In this model, availability of neurons for synchronization is decreased in conjunction with increase in the excitability level of neurons, resulting amplitude attenuation of EEG oscillations. Simultaneous EEG-fMRI measurements extended this model by showing that the changes in motor imagery- and actual movement-induced ERD and the BOLD signal co-localized at the sensorimotor area, and the magnitude of ERD and BOLD co-varied (Formaggio *et al*., 2008, 2010; Ritter *et al*., 2009; Yuan *et al*., 2010). Hummel *et al*. (2002) also reported empirical evidence of a concurrent increase of MEPs induced by the single pulse TMS over M1 and sensorimotor

ERD at 11–13 Hz during motor imagery. More recently, a negative correlation between the MEP amplitude and sensorimotor EEG amplitude in the alpha or beta band was shown by using simultaneous TMS-EEG studies (Mäki and Ilmoniemi, 2010; Sauseng *et al*., 2009). ERD during motor imagery is therefore believed to represent increased activation of the sensorimotor area. However, it still remains unclear (1) whether the M1 excitability co-varies with ERD recorded over the sensorimotor area, and (2) what parts of the intracortical circuits involved in motor output change their activity in conjunction with ERD during motor imagery.

There are several reasons why these two issues described above remain outstanding. For example, the BOLD signal is inferior in time resolution (2–3 s (Poldrack *et al*., 2011)) compared with the alpha and beta bands in EEG (in the order of 100 ms). Further, the BOLD signal indicates hemodynamic cortical activity, but not necessarily electric cortical excitability. MEP amplitude induced by the single pulse TMS indicates the corticospinal excitability, although it cannot document the independent excitabilities of the M1 and spinal motoneurons.

The present study used the paired pulse TMS technique to assess changes in SICI and ICF within M1 related to ERD during motor imagery. In the previous studies, a negative correlation between MEP amplitude and amplitude of the sensorimotor EEG oscillation was demonstrated using at least 60 times of single pulse TMS (Mäki and Ilmoniemi, 2010; Sauseng *et al*., 2009). This implies the difficulty in using the same protocol for the present study because of the large number of magnetic stimuli. Thus, I examined the relationship between ERD magnitude (calculated from online EEG) and M1 excitability using single and paired pulse TMS, which was triggered by the instantaneous ERD magnitude, in three different predetermined ERD magnitudes. ERD-triggered TMS may require fewer stimuli

than the non-triggered TMS.

The purpose of the study presented in Chapter 2 was to assess the association of sensorimotor EEG changes reflected by an ERD with M1 excitability during motor imagery of wrist movements using single and paired pulse TMS, and to determine what parts of the intracortical circuits involved in motor output change their activity following ERD during wrist motor imagery from the outcomes of SICI and ICF. The difference in the association of ERD during motor imagery of agonist muscle contraction with the corticospinal excitability modulation to the wrist flexor and extensor was also examined. It is because contrasting results have been shown on the corticospinal excitability modulation to the wrist flexor and extensor muscles induced by the agonist contraction (Chye *et al*. 2010; Izumi *et al*. 2000; McMillan *et al*., 2004) and the motor imagery of agonist contraction (Levin *et al*., 2004).

2.2 Materials and Methods

2.2.1 Participants

Twenty healthy participants (aged 21.8 ± 1.2 years; 15 males, 5 females) joined this study. All were right-handed, without any medical or psychological disorders, and had normal vision (according to self-reports). All participants were initially naive to the experiment. The purpose and experimental procedure were explained to the participants, and written informed consent was obtained. The study was approved by the institutional ethics review board (#23-16) and performed in accordance with the Declaration of Helsinki.

2.2.2 Data Acquisition

EEG was recorded from five Ag/AgCl electrodes of 10 mm in diameter placed at C3 and 2 cm anterior (C3a), posterior (C3p), medial (C3m) and lateral (C3l) to C3 to cover the contralateral hand sensorimotor area (Fig. 2-1a). In two randomly selected participants, an additional 18 electrodes were placed over the whole head for verification of spatial configuration of ERD during wrist motor imagery, and which confirmed the observed ERD during wrist motor imagery (Fig. 2-1b). Impedance for all channels was maintained below 10 kΩ throughout the experiment. EEG signals were band-pass filtered (0.1–256 Hz with 2nd order Butterworth) with a notch (50 Hz for avoiding power line contamination), and digitized at 512 Hz using a biosignal amplifier (g.USBamp; Gouger Technologies, Graz, Austria).

Surface EMG activity was recorded from the right flexor carpi radialis (FCR) or extensor carpi radialis (ECR) muscle by using bipolar Ag/AgCl electrodes of 10 mm in diameter. The cathode electrode was placed over the belly of the FCR or ECR muscle and the anode electrode was placed 20 mm distal from the cathode electrode. Impedance for all channels was maintained below 20 kΩ throughout the experiment. EMG signals were band-pass filtered (5–1000 Hz with 2nd order Butterworth) with a notch (50 Hz for avoiding power line contamination), digitized at 2 kHz using a biosignal amplifier (Neuropack MEB-9200; Nihon Kohden, Tokyo, Japan), and monitored throughout the experiment. Recording of each trial started 50 ms prior to the TMS pulse and finished after 150 ms.

TMS was applied using a figure-of-eight shaped coil (outer diameter of each coil: 7 cm) connected to the Magstim 200 magnetic stimulator (Magstim; Whiteland, UK). To apply paired pulse, two stimulators connected by the Bistim module (Magstim) were used.

The optimal coil position where MEPs in FCR or ECR muscle could be evoked with the lowest stimulus intensity was marked with ink to ensure an exact repositioning of the coil throughout the experiment. Identification of the optimal coil position was performed prior to each experimental condition. At this coil position, the motor threshold intensity was defined as the lowest stimulator output intensity capable of inducing an MEP of at least 50-μV peak-to-peak amplitude in relaxed muscles in at least half of the 10 trials (Rossini *et al*., 1994). Stimulus intensities are expressed as a percentage of the maximum stimulator output. Single pulse TMS was applied with an intensity of 120% of the individual motor threshold. Paired pulse TMS was used to investigate SICI and ICF. A subthreshold conditioning stimulus was set at 80% of the motor threshold, and was delivered through the same magnetic coil at 2 or 3 and 10 or 15 ms prior to the suprathreshold test stimulus adjusted to 120% of the motor threshold. The stimulus intensity remained constant throughout the whole experiment for each subject.

2.2.3 Experimental Protocol

The participants were randomly assigned one of two conditions: kinesthetic motor imagery of sustained wrist extension and kinesthetic motor imagery of sustained wrist flexion. Surface EMG was recorded from the agonist muscle of imagined movement. Each participant participated in a series of four experimental sessions in the following order: Screening session, TMS Conditions 1, 2 and 3. The screening session and TMS Conditions 1, 2 and 3 were performed on the same day.

In the screening session, the participant sat in a comfortable armchair, put their hand with palm side down on the table and performed kinesthetic motor imagery of sustained wrist extension or wrist flexion in the fixed repetitive time scheme (Fig. 2-1c). A 20-inch

computer monitor was placed 60 cm in front of the participants' eyes. Each trial started with the presentation of the word 'Rest' at the upper left of the monitor. Six seconds later, the word 'Ready' was presented for 1 s. The participant was then asked to perform motor imagery of wrist extension or wrist flexion for 5 s. The monitor showed the word 'Image' during motor imagery. After a short pause, the monitor shows the word 'Rest', and the next trial started. Screening session consisted of 20 trials.

TMS Condition 1 was conducted as a control for TMS Conditions 2 and 3. I applied single and paired pulse TMS (ISIs; 2 or 3 and 10 or 15 ms) to the contralateral hand M1 during the rest condition. The background EMG activity was monitored during the experiment, and trials contaminated by more than ±20 μV in background EMG activity were discarded. Each stimulus was applied at least ten times in random order at intervals of 6 s ± 500 ms, and fifty MEPs were collected in this session. In TMS Conditions 2 and 3, I used the ISIs obtained during TMS Condition 1 that showed a strong effect on SICI and ICF, respectively.

TMS Condition 2 was performed using the same time scheme as the screening session (Fig. 2-1c). A continuously moving feedback bar was displayed on the center of the screen during motor imagery. This feedback bar appeared after the task cue, and was presented for a 5 s period. According to the ERD or ERS magnitude (band power decrease or increase) caused by the required motor imagery, the feedback bar in the screen was continuously moving. The feedback bar changed its length in a linear fashion from the center to the right and left edge of the monitor, corresponding to 0% to 30% of the ERD and ERS, respectively. The participants' task was to extend the bar horizontally toward the right edge of the monitor at maximal voluntary effort. The participants were informed that a successful wrist motor imagery would shift the bar to the right, and an unsuccessful wrist

motor imagery would shift the bar to the left. The methods to calculate ERD and the online algorithm for controlling the length of bar extension in the screen are described below (*2.2.4 Electroencephalogram Analysis*). I applied either single or paired pulse TMS, with an ISI of 2 or 3 ms or an ISI of 10 or 15 ms, to the contralateral hand M1 on the first instance the ERD exceeded 5% during motor imagery (Fig. 2-1d). The background EMG activity was monitored during the experiment, and trials contaminated by more than ±20 μV in background EMG activity were discarded. Each stimulus was applied ten times in a random order, and MEPs were collected.

To minimize the effect of slow intrinsic oscillations around 0.1 Hz (Mayer waves) in blood pressure, heart rate and (de)oxyhemoglobin on the excitability level in the brains' motor areas (Pfurtscheller *et al*., 2012), TMS Condition 3 was performed using the same conditions as in TMS Condition 2, except that TMS was applied immediately after ERD exceeded 15% during motor imagery.

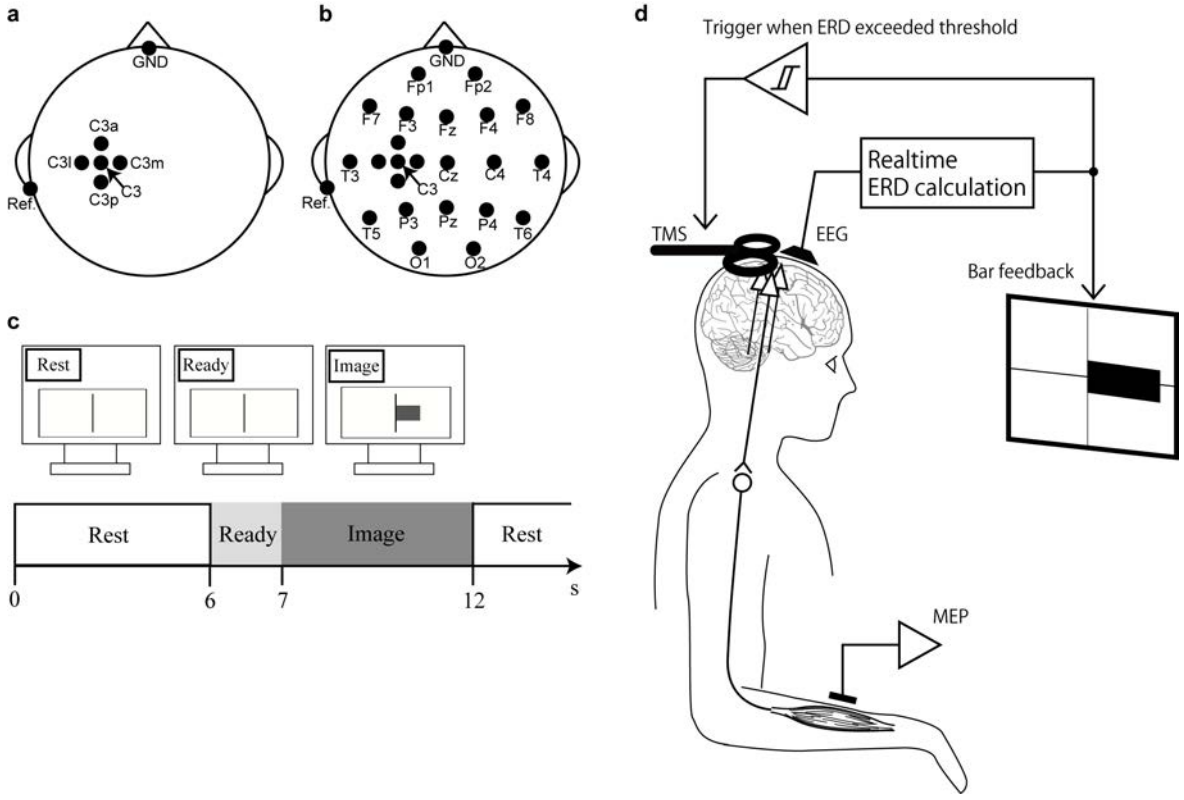

Figure 2-1. Experimental setup and paradigm

(a) In 18 participants, five EEG electrodes were placed to cover around the right hand sensorimotor area, as designated according to the International 10–20 System, and 2 cm anterior, posterior, medial and lateral to C3 (termed C3a, C3p, C3m and C3l, respectively). (b) In two participants, 23 EEG electrodes were placed over the whole head, as designated according to the International 10–20 System, and 2 cm anterior, posterior, medial and lateral to C3. The ground electrode (GND) was placed over the forehead, and the reference electrodes (Ref) were located at the left earlobe. (c) Timing of the paradigm used in the screening session and TMS Conditions 2 and 3. (d) Experimental system of the TMS Conditions 2 and 3.

2.2.4 Electroencephalogram Analysis

EEG data were segmented into successive 512-point (1,000 ms) windows with 480-point overlapping. A fast Fourier transformation with a Hanning window was applied to each segment. Power spectrum density was estimated from the square of the absolute value of the fast Fourier transformation, and ERD was defined as a decrease in the power spectrum compared with a reference period, defined as the interval from -3 s to the time 'Ready' was displayed on the monitor. Thus, ERD was calculated with a time resolution of 62.5 ms and a frequency resolution of 1 Hz during each 5-s task period, according to the following equation.

$$ERD(f,t) = \frac{R(f) - A(f,t)}{R(f)} \times 100\%,$$

where $A(f,t)$ is the power spectrum density of the EEG at time *t* with the onset of motor imagery and frequency *f*, and $R(f)$ is the mean power spectrum of the reference intervals. This equation expresses a large ERD as a large positive value. ERD was typically found over the sensorimotor area contralateral to the imagery hand, but the most reactive frequency band displaying ERD and its spatial characteristics are slightly different for each participant (Pfurtscheller *et al*., 2006). I determined the best electrode setup and frequency band within alpha and beta bands in the screening session with each participant. Pairs of C3 and 2 cm anterior, posterior, medial and lateral to C3 bipolar EEG signals were used to check existence of ERD during wrist motor imagery, and to define the electrode pair and the 3 Hz width frequency band displaying the largest ERD. Herein, this frequency band is referred to as 'the most reactive frequency band displaying ERD (Pfurtscheller *et al*. 2006)'. The electrode pair and the frequency band that displayed the strongest ERD were used for online ERD calculations in TMS Conditions 2 and 3. To avoid sudden movements

of the feedback bar, the moving bar feedback was updated every segment (62.5 ms) by an averaged ERD of the last 16 segments (1,000 ms).

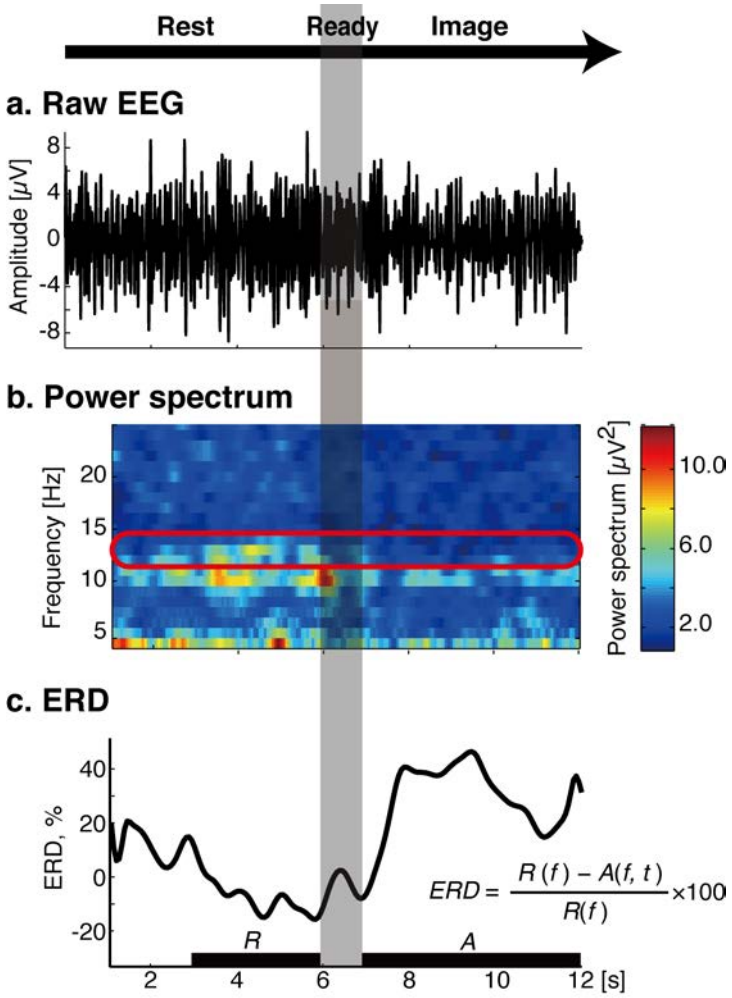

Figure 2-2. Method for ERD analysis

(a) EEG was segmented into successive 512-point (1,000 ms) windows with 480-point overlapping. (b) The fast Fourier transform with the Hanning window was applied in each segment to calculate the time course of power spectrum of EEG. (c) The power was normalized with reference to the period from 3 to 6 s, referred to as *R*. The ERD magnitude was calculated every 62.5 ms with 3 Hz width frequency band (which is illustrated by the red box of Fig. 2-2b), showing the strongest ERD.

In the offline analysis, two participants whose EEG signals were obtained from 23 electrodes were used to reconstruct the topographical brain images of ERD magnitude. Nineteen channels of the EEG signals (excluding the 2 cm anterior, posterior, medial and lateral to C3) were re-referenced using a four neighbors Laplacian spatial filter (Hjorth, 1975). All EEG trials were visually controlled for artifacts and were discarded in cases of artifact-contaminated trials. ERD was then calculated from a 1-s EEG epoch prior to the magnetic stimulation compared with the baseline period. Since TMS Condition 1 was a resting condition, I used the interval from 1.5 to 4.5 s of each trial as the baseline period of TMS Condition 1. Baseline period of TMS Conditions 2 and 3 were the same interval as the online analysis. Spatially interpolated topographic ERD maps were plotted in accordance with their channel locations over the scalp using trial average of ERD magnitudes just prior to the magnetic stimulation. Both moving bar feedback and all off-line analysis were performed by MATLAB 2010a (MathWorks, Natick, MA).

2.2.5 Motor Evoked Potential Analysis

Each single sweep was inspected visually, and the trials with artifacts (pre-stimulus EMG activity more than ±20 μV) were rejected. The artifact-free MEP amplitudes were then measured peak-to-peak. Paired pulse TMS was performed to investigate SICI and ICF, which were expressed as a percentage of the ratio between the conditioned MEPs and the unconditioned MEPs (mean conditioned MEP / mean unconditioned MEP × 100). Herein, this value is referred to as %unconditioned MEP, where 100 in %unconditioned MEP indicates absence of facilitation or inhibition, while values more than 100 and less than 100 in %unconditioned MEP indicate facilitation and inhibition, respectively. The peak-to-peak amplitudes and %unconditioned MEP were analyzed with Bistim Tracer (Medical Try

System, Tokyo, Japan).

2.2.6 Statistical Tests

One-way analysis of variance (ANOVA) with repeated measures was used to determine the effect of experimental conditions (TMS Conditions 1, 2, and 3) on MEP amplitudes induced by single pulse TMS and %unconditioned MEP of SICI and ICF and averaged EEG power values for the reference period, which was calculated with the bipolar channel and the frequency band displaying largest ERD as shown in Table 1. If ANOVA yielded a significant F value, Tukey's post-hoc test was performed. Type I error was set to 0.05.

2.3 Results

2.3.1 Spectral Power of Electroencephalogram

In the screening session, all participants showed the ERD during right wrist motor imagery around C3 (Fig. 2-3a: an example obtained from participant 1A). The characteristics of ERD such as the most reactive frequency band and bipolar channels in the screening session are summarized in Table 2-1. The frequency band displaying the largest ERD was not different between participants who performed motor imagery of wrist flexion and extension ($t_{18} = 0.31$, $P > .05$).

One-way ANOVA was performed in the most reactive frequency band displaying ERD of each participant with regard to power values during the reference period in TMS Conditions 2 and 3 and during 1.5-4.5 s of each trial in TMS Condition 1, which correspond to the reference period in TMS Conditions 2 and 3. There was no significant difference in the reference power values between TMS Conditions 1, 2 and 3 in both the experimental group of EMG recording from the FCR muscle ($F_{2, 18} = 0.20$, $P > .05$) and the ECR muscle ($F_{2, 18}$

= 0.10, $P > .05$). This indicated similar means of reference power values for the resting and motor imagery conditions.

Figure 2-4a represents the ERD topographic maps in the TMS Conditions 1 (at rest), 2 (at ERD 5% during right wrist motor imagery) and 3 (at ERD 15% during right wrist motor imagery) from the 19-channel EEG signals of participant 1A. The colors on the topographic maps indicate ERD magnitudes calculated from the four neighbors Laplacian deviation of the EEG signals. The ERD magnitudes of the maps were constructed from the most reactive frequency band displaying ERD in the screening session, as shown in Table 1. Results showed that ERD magnitude at C3 in the experimental condition of ERD 15% was stronger than that of ERD 5% (27.2% and 6.9%, respectively). In addition, ERD magnitude at Cz was the second largest in the experimental condition of ERD 15%, while the ERD magnitude at P3 was the second largest in the experimental condition of ERD 5% (16.9% and 4.8%, respectively). Participant 1B also showed that ERD magnitudes at C3 were the largest in the both experimental conditions of ERD 5% and 15% (25.6% and 8.4%, respectively). These data indicate that the observed ERD during right wrist imagery was likely to localize at the contralateral sensorimotor area in this experimental procedure. The other 18 participants were recorded EEG from 5 channels over the contralateral sensorimotor area for the convenience of the experimental duration using TMS.

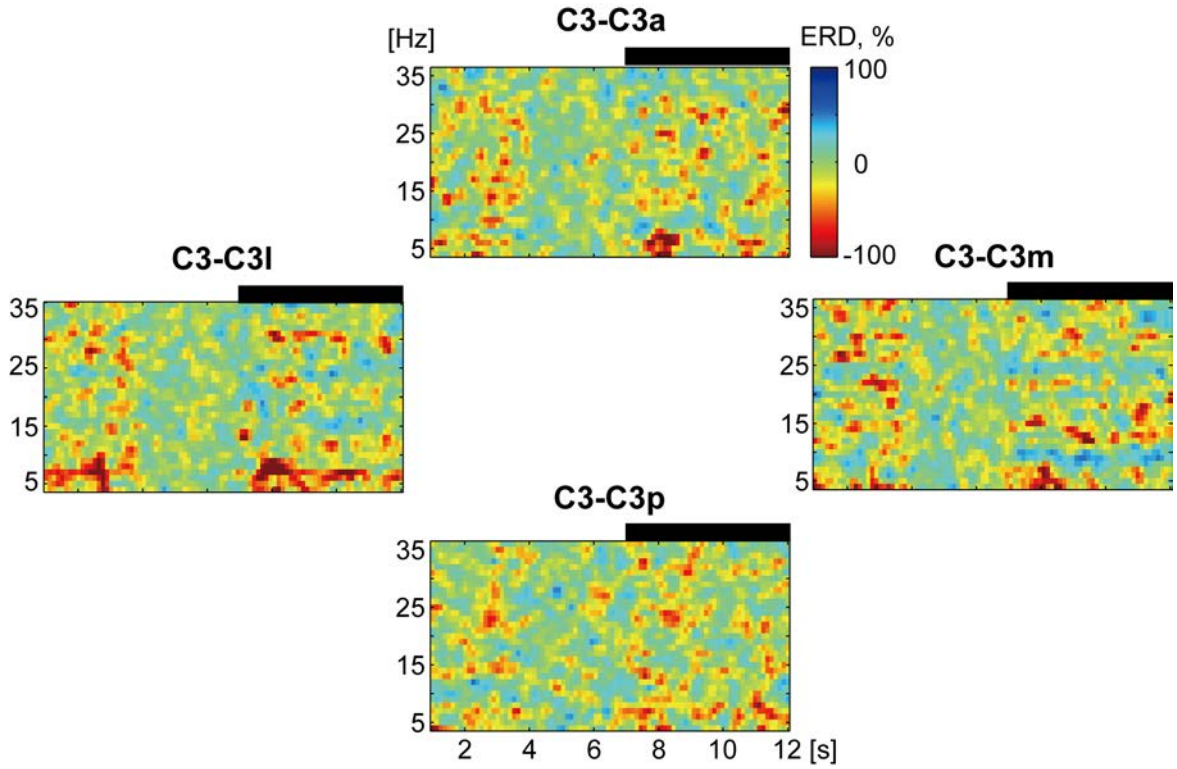

Figure 2-3. ERD time-frequency map in the screening session

Data was obtained from participant 1A. Black bar at the upper right of each map indicates the time period of motor imagery. The most reactive frequency band and bipolar channels displaying ERD were 9–11 Hz and C3-C3m, respectively.

Table 2-1. Frequency band and bipolar channel displaying the largest ERD during right wrist motor imagery in the screening session

Participant	Imagery task	Channel	Frequency [Hz]
1A	wrist extension	C3-C3m	9–11
1B	wrist extension	C3-C3m	8–10
1C	wrist flexion	C3-C3l	13–15
1D	wrist flexion	C3-C3a	10–12
1E	wrist extension	C3-C3a	16–18
1F	wrist extension	C3-C3l	10–12
1G	wrist extension	C3-C3a	8–10
1H	wrist flexion	C3-C3p	10–12
1I	wrist extension	C3-C3m	12–14
1J	wrist extension	C3-C3p	10–12
1K	wrist flexion	C3-C3p	17–20
1L	wrist flexion	C3-C3a	10–12
1M	wrist flexion	C3-C3p	8–10
1N	wrist flexion	C3-C3l	7–9
1O	wrist flexion	C3-C3p	9–11
1P	wrist flexion	C3-C3p	20–22
1Q	wrist extension	C3-C3p	16–18
1R	wrist extension	C3-C3p	12–14
1S	wrist extension	C3-C3p	8–10
1T	wrist flexion	C3-C3p	10–12

2.3.2 Changes of the Intracortical Excitability

Figure 2-4b shows MEP responses of the agonist muscle of motor imagery in all experimental conditions from participant 1A. MEP amplitudes evoked by the single pulse TMS were facilitated during motor imagery (Rest = 0.556 mV, motor imagery at ERD 5% = 1.035 mV, motor imagery at ERD 15% = 1.417 mV). As an increase in

the %unconditioned MEP reflects both ‘reduced SICI’ and ‘increased ICF’, both SICI and ICF were reduced in accordance with the ERD magnitude (SICI: Rest = 16.1%, motor imagery at ERD 5% = 36.7%, motor imagery at ERD 15% = 59.9%; ICF: Rest = 231%, motor imagery at ERD 5% = 185%, motor imagery at ERD 15% = 158%). Furthermore, the increase of MEP amplitudes induced by the single pulse TMS and SICI was related to ERD magnitude.

Figure 2-5a represents MEP amplitudes induced by the single pulse TMS, SICI and ICF from the FCR muscle in the resting condition during motor imagery of right wrist flexion at ERD 5% and ERD 15%. One-way ANOVA showed that the effect of ERD for MEP amplitudes ($F_{2, 18} = 14.5$, $P < .001$) and SICI ($F_{2, 18} = 4.01$, $P < .05$) were statistically significant, but not for ICF ($F_{2, 18} = 0.06$, $P > .05$). Post-hoc test revealed that MEP amplitudes were significantly larger at ERD 5% ($P < .01$) and ERD 15% ($P < .001$) compared with the resting condition. SICI was significantly reduced at ERD 15% compared with the resting condition ($P < .01$), and tended to reduce at ERD 15% compared with ERD 5% ($P = .068$).

Figure 2-5b represents the MEP amplitudes induced by the single pulse TMS, SICI and ICF from the ECR muscle in the resting condition during motor imagery of right wrist extension at ERD 5% and ERD 15%. One-way ANOVA showed that the effect of ERD for MEP amplitudes ($F_{2, 18} = 6.44$, $P < .01$) and SICI ($F_{2, 18} = 11.8$, $P < .001$) were statistically significant, but not for ICF ($F_{2, 18} = 0.90$, $P > .05$). Post-hoc test revealed that MEP amplitudes were significantly larger at ERD 5% ($P < .05$) and ERD 15% ($P < .01$) compared with the resting condition. SICI was significantly reduced at ERD 15% compared with both conditions of rest ($P < .001$) and ERD 5% ($P < .05$). The results of TMS measurements were summarized into Table 2-2.

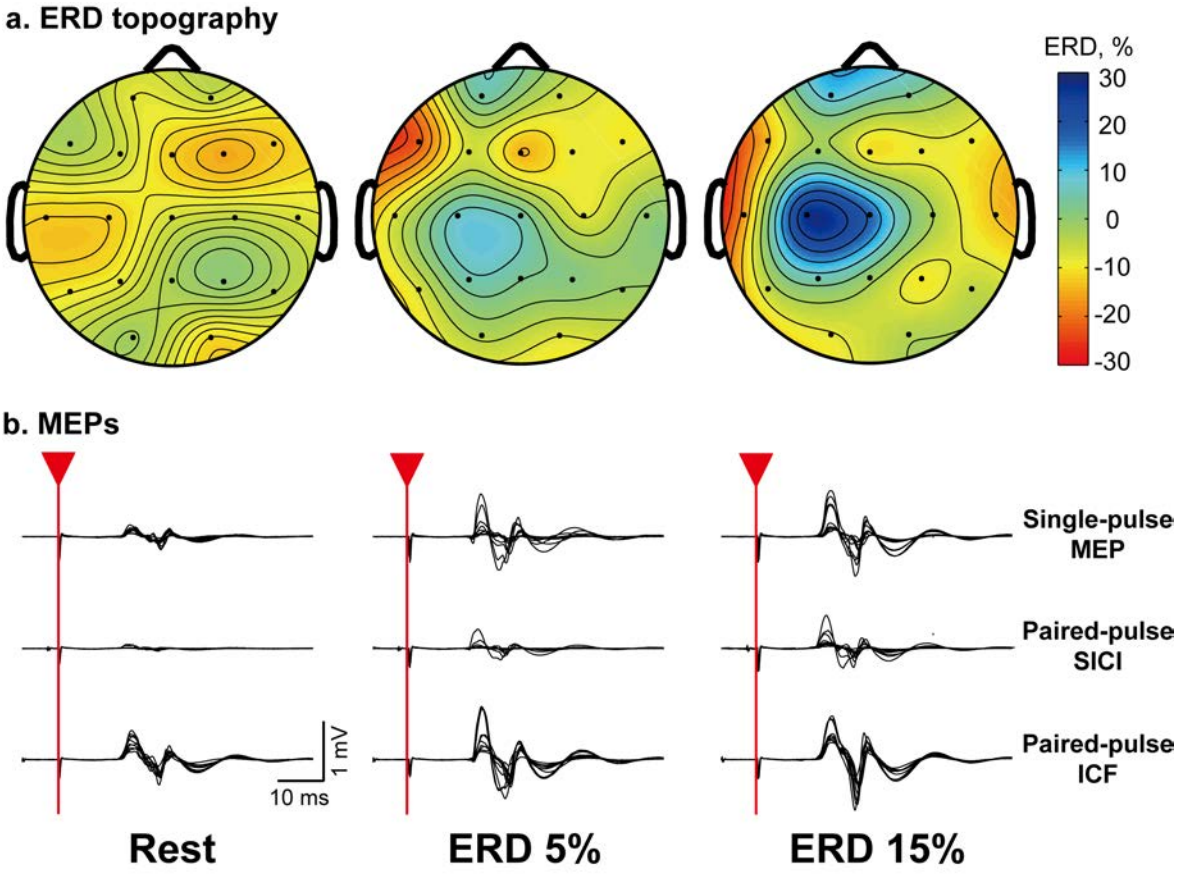

Figure 2-4. ERD topographies and MEP traces in one representative participant (Participant 1A)

(a) ERD topographies were constructed from the 19-channel EEG data in the resting condition, and during motor imagery of the right wrist extension at ERD 5% and 15%. Topographic maps are illustrated in the frequency range of 9–11 Hz, which was the most reactive frequency band displaying ERD of participant 1A. Electrode positions are shown by dots. Positive values (blue colors) indicate strong ERD. (b) MEP traces induced by the single and paired pulse TMS in the resting condition, and during motor imagery of the right wrist extension at ERD 5% and ERD 15%. MEPs were recorded from the ECR muscle. Ten MEP traces were overlaid per condition. The red triangles and vertical lines indicate the timing of stimulus. Single-pulse MEP amplitude was markedly increased during motor imagery, and SICI and ICF were markedly reduced as the ERD increased.

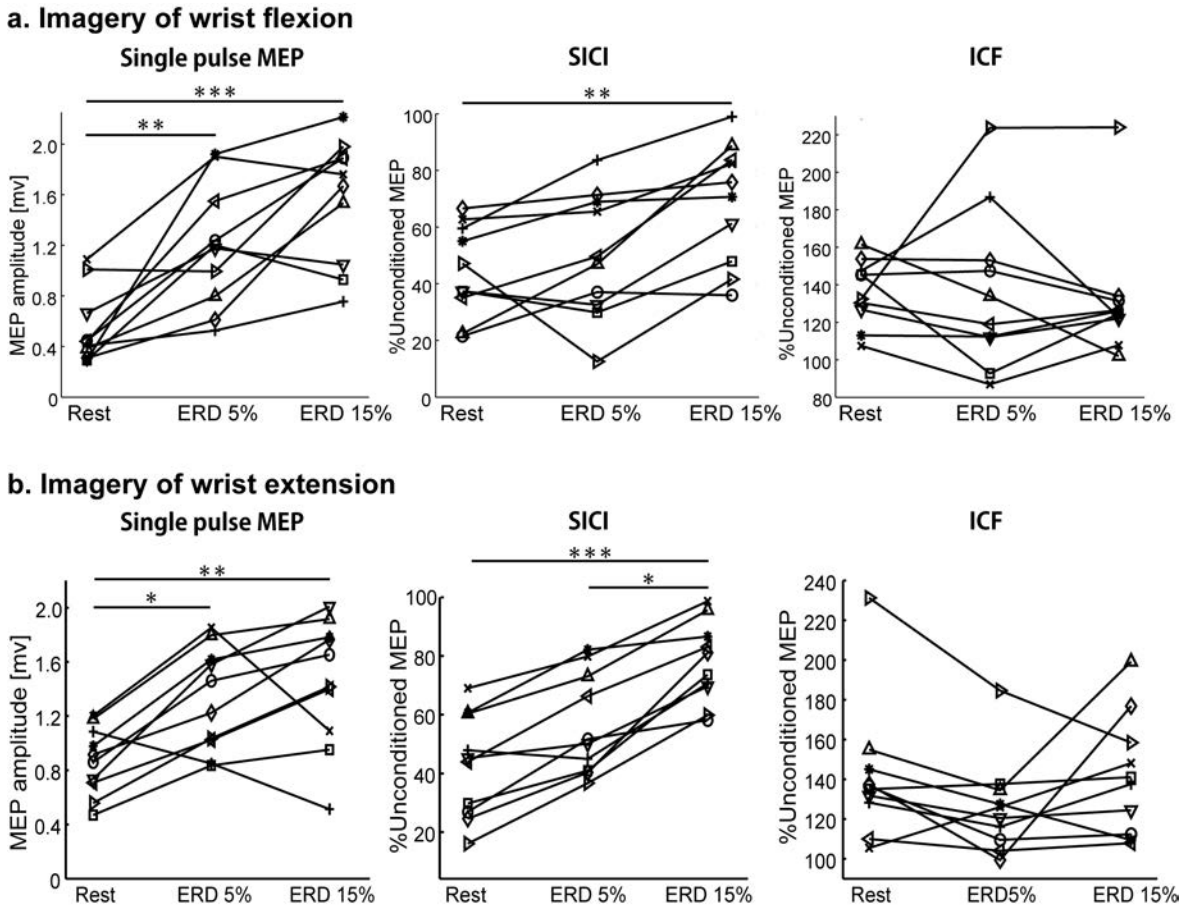

Figure 2-5. MEP amplitude, SICI, and ICF in the resting condition and during wrist motor imagery at ERD 5% and 15%

(a) MEP amplitudes induced by the single pulse TMS, SICI, and ICF recorded from FCR muscle in the resting condition, and during motor imagery of wrist flexion at ERD 5% and 15%, and (b) those of recorded from ECR muscle in the resting condition, and during motor imagery of wrist extension at ERD 5% and 15%. Each line shows the result obtained from each participant. * $P < .05$, ** $P < .01$, *** $P < .001$.

Table 2-2. TMS measurements in the resting condition, and wrist motor imagery at ERD 5% and 15%

		Agonist muscle of the motor imagery task	
		FCR	ECR
Single pulse MEP [mV]	Rest	0.533 ± 0.293	0.869 ± 0.252
	ERD 5%	1.191 ± 0.488	1.327 ± 0.383
	ERD 15%	1.566 ± 0.492	1.449 ± 0.476
SICI, %	Rest	44.5 ± 16.2	42.4 ± 17.7
	ERD 5%	49.8 ± 22.3	56.6 ± 17.2
	ERD 15%	68.7 ± 21.3	77.7 ± 13.8
ICF, %	Rest	136 ± 17.5	141 ± 34.8
	ERD 5%	136 ± 42.7	126 ± 24.1
	ERD 15%	132 ± 33.8	141 ± 30.2

Values represent mean ± SD.

I further investigated whether the intracortical excitability is correlated with the ERD magnitude in different frequency bands. According to the previous studies, specific ERD frequency band, such as alpha (7–13 Hz) and beta (14–26 Hz), is likely to exhibit stronger association with the intracortical excitability. Figure 2-6 illustrated correlations between SICI and ERD values in different frequency ranges (i.e., alpha, beta, and the most reactive frequency band displaying ERD in the screening session). ERD was calculated with 1-s EEG data prior to the nerve stimulation derived from the electrode pair displaying the largest ERD in the screening session. Participants who performed motor imagery of wrist flexion (Fig. 2-6a) showed significant correlation in the most reactive frequency band displaying ERD ($r_{18} = 0.45$, $P < .05$), but not with alpha or beta band. On the other hand, participants who performed motor imagery of wrist extension (Fig. 2-6b) showed that SICI was significantly correlated with the ERD magnitude in not only the most reactive

frequency band displaying ERD (r_{18} = 0.76, P < .001), but also alpha (r_{18} = 0.47, P < .05) and beta bands (r_{18} = 0.59, P < .01).

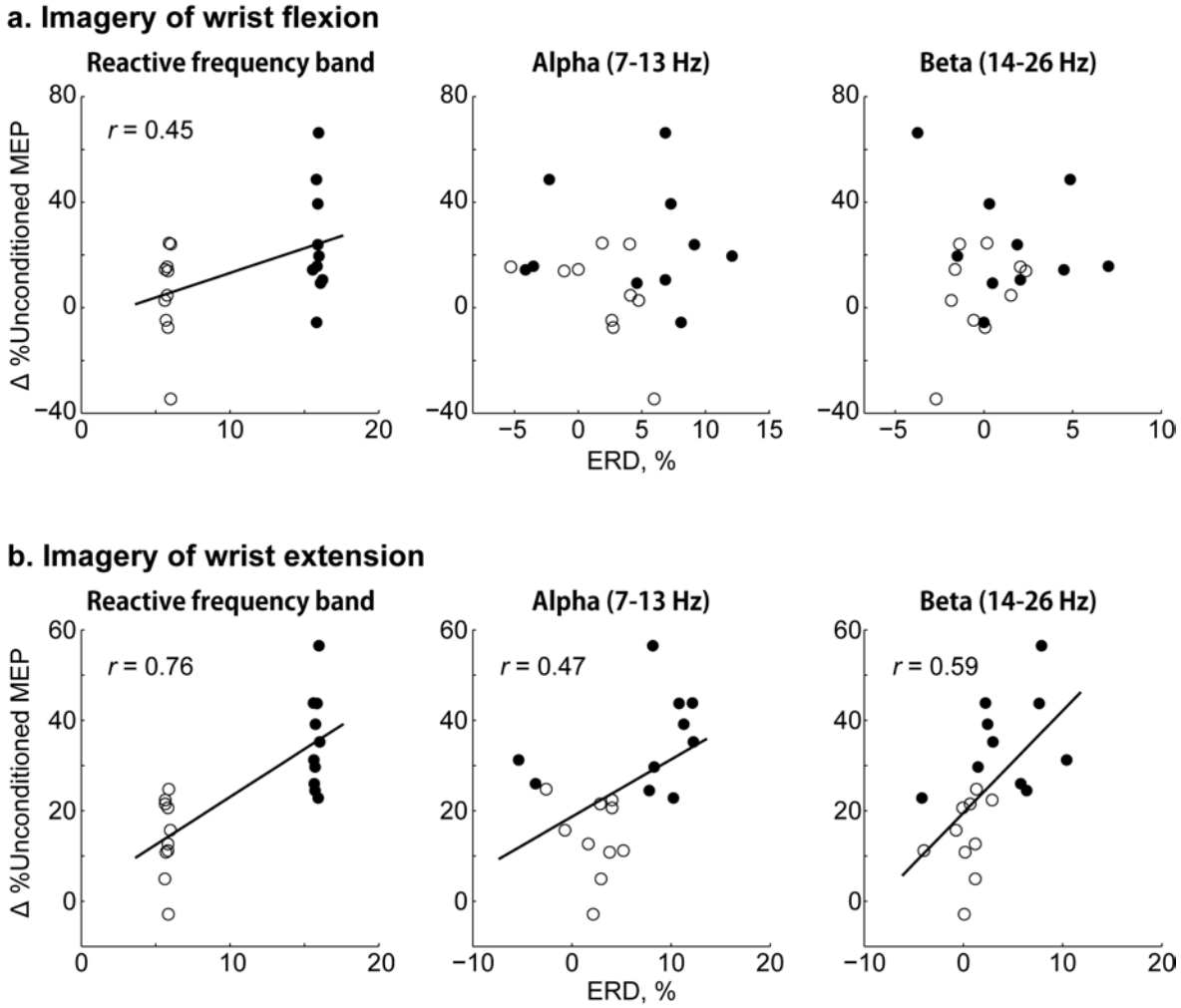

Figure 2-6. Relationship between the ERD frequency band and SICI during motor imagery of wrist flexion and wrist extension

X-axis represents the averaged ERD value calculated with the 1-s bipolar EEG data prior to stimulation, in the frequency range of the most reactive frequency bands displaying ERD, 7–13 Hz (alpha), and 14–26 Hz (beta). Positive values indicate strong ERD. Y-axis represents subtraction of the percentage of SICI in TMS Conditions 2 and 3 from TMS Condition 1. Open and filled circles reflect data from TMS Conditions 2 and 3, respectively.

2.3.3 Effects of Task Compliance on Intracortical Excitability

The relationship between SICI, an index of the intracortical excitability, and the task success rate, an index of task difficulty, was examined. Task success was defined as when the EEG power in a certain frequency band decreased 5% or 15%, relative to the baseline period, during the 5-s motor imagery period in TMS Conditions 2 and 3, respectively. The percentage of task success in TMS Conditions 2 and 3 were 54.1 ± 9.1% and 30.9 ± 5.4% in the motor imagery task of wrist flexion (t_9 = 8.93, P < .001) and 51.3 ± 14.1% and 29.1 ± 4.0% in the motor imagery task of wrist extension (t_9 = 4.81, P < .001), respectively. I further compared the correlation between SICI and percentage of task success (Fig. 2-7a), but these were not statistically significant for both the wrist flexion imagery and the wrist extension imagery (P > .05).

Time duration of the motor imagery before magnetic stimulation was also compared. The results in TMS Conditions 2 and 3 were 1.54 ± 0.21 s and 3.05 ± 0.22 s in the motor imagery task of wrist flexion (t_9 = 18.3, P < .001) and 1.63 ± 0.22 s and 3.07 ± 0.13 s in the motor imagery task of wrist flexion (t_9 = 23.3, P < .001). The correlation between SICI and the time duration of the motor imagery was significant for the wrist extension imagery (r_{18} = 0.78, P < .001) but not for the wrist flexion imagery (P > .05).

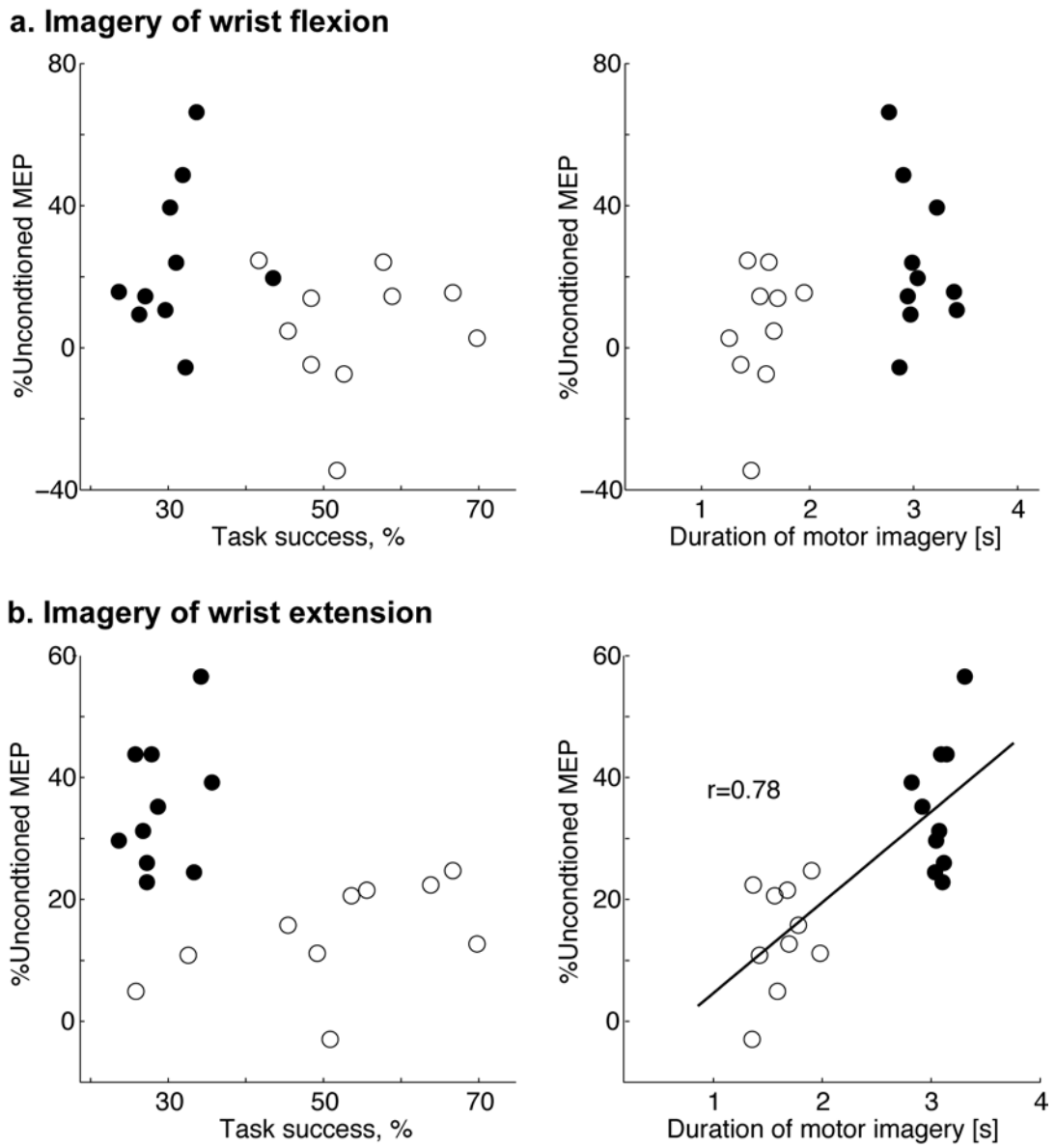

Figure 2-7. Correlation between SICI, percentage of task success, and duration of the motor imagery before stimulation

Results obtained from participants who performed motor imagery of wrist flexion (a) and wrist extension (b). In the left panels, X-axis represents the percentage of task success. In the right panels, X-axis represents the time duration of motor imagery. Y-axis represents subtraction of the percentage of SICI in TMS Conditions 2 and 3 from TMS Condition 1. Open and filled circles reflect data from TMS Conditions 2 and 3, respectively.

2.4 Discussion

2.4.1 Relationship between Sensorimotor Event-Related Desynchronization and Intracortical Excitability

The purpose of this study was to examine the physiological relationship between motor imagery-induced EEG changes (termed ERD) and cortical excitability using paired pulse TMS, which was contingent on the instantaneous ERD magnitude. I found that the magnitude of ERD during right wrist motor imagery was associated with a significant increase in MEP amplitudes and a significant decrease in SICI, but no significant changes were found in ICF.

Numerous studies have examined the changes of corticospinal excitability during wrist or hand motor imagery by using single pulse TMS, and have reported that wrist/hand motor imagery significantly increases corticospinal excitability (Kasai *et al*., 1997; Patuzzo *et al*., 2003; Rossi *et al*., 1998; Rossini *et al*., 1999; Stinear *et al*., 2006; Yahagi and Kasai, 1998). Patuzzo *et al*. (2003) showed that SICI was significantly reduced during hand motor imagery, but not ICF. The present results are in agreement with those studies. ERD during right wrist motor imagery led to a significant increase in MEP amplitudes induced by single pulse TMS and significant decrease in SICI, but not ICF. In addition, and most importantly, I found that the increase of MEP amplitudes and the reduction of SICI were positively related to the increase of ERD magnitude. While MEP amplitude induced by single pulse TMS is thought to be related to the contralateral corticospinal excitability, SICI and ICF seem to reflect the excitability of distinct inhibitory and excitatory interneuronal circuits within M1 (Chen *et al*., 1998; Chen, 2004; Kujirai *et al*., 1993). As it was reported that $GABA_A$ agonists enhance SICI (Ziemann *et al*., 1996) and *N*-methyl-D-aspartame antagonists abolish ICF (Ziemann *et al*., 1998), I suggest that ERD

magnitude during motor imagery is associated with an increase in the contralateral M1 excitability, which is mediated by a down-regulation of GABAergic activity.

I noted here that the MEP amplitude in response to the test stimulus was different between the experimental conditions; i.e., the MEP amplitude in TMS Condition 3 (wrist motor imagery at ERD 15%) was significantly larger than that of TMS Condition 1 (resting condition). One concern is that the decrease in the amount of SICI was influenced by the increase of the test MEP amplitude rather than changes in the activity of GABAergic neurons. However, whereas Sanger *et al.* (2001) reported a positive correlation between the amount of SICI and MEP amplitude, the present results showed a reduction of SICI with an increase of MEP amplitude. Therefore, reduction of SICI in the present study likely reflects down-regulation of GABAergic activity in the M1.

In TMS Conditions 2 and 3, MEP was recorded in a largely different condition as compared with rest (TMS Condition 1). The subjects were asked to perform motor imagery and received online feedback of their own ERD modulation. According to this protocol, the observed MEP increase and SICI change were likely to be related to the motor imagery task and neurofeedback context. Ono *et al.* (2013) illustrated that motor cortical excitability was significantly lesser in the no visual feedback condition than when the visual feedback of ERD values were provided. Thus, the MEP increase and SICI decrease in TMS Conditions 2 and 3 compared to TMS Condition 1 could be modulated by both the motor imagery task and feedback context. On the other hand, the difference between TMS Conditions 2 and 3 was solely in the ERD magnitude at the time of magnetic stimulation. Overall, the present study indicated that while the increase in the MEP amplitude (i.e., the corticospinal excitability) could be related to both the motor imagery task and neurofeedback context, the decrease in SICI (i.e., downregulation of inhibitory interneurons activity) was predominantly related to

the ERD magnitude during motor imagery.

Since SICI was not related to the percentage of task success, an increase in the cortical excitability would not be associated with the task difficulty. In contrast, SICI of ECR muscle was correlated with the duration of motor imagery of wrist extension. SICI of FCR muscle also showed a moderate correlation with the duration of motor imagery of wrist flexion. As shown in Fig. 2-8, a longer duration of motor imagery would be required for generating a larger ERD. One limitation on investigating the relationship between ERD and cortical excitability is the difficulty in eliminating the effect of motor imagery period.

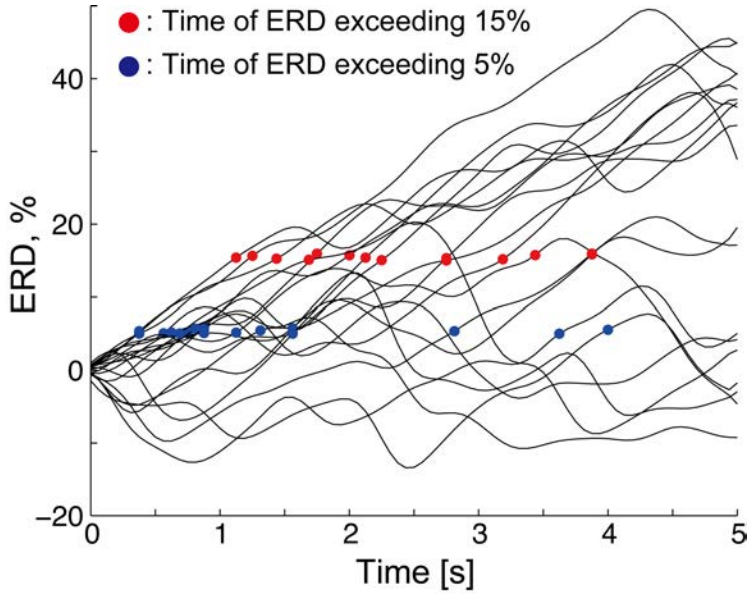

Figure 2-8. An example of an ERD time course during the motor imagery task

Data was obtained from participant 1R in the screening session. X-axis represents the time from the onset of the motor imagery task. Red and blue circles reflect the time of ERD exceeding 15% and 5%, respectively. The participant performed the motor imagery task 20 times, and ERD exceeded 15% 14 times and 5% 19 times. It can be seen that a longer duration of motor imagery is required for generating a larger ERD.

The present results are also comparable to previous reports investigating changes in cortical excitability during human voluntary movement. MEPs in response to single pulse TMS were strongly augmented in a period of 90–100 ms before the onset of voluntary EMG activity (Nikolova *et al.*, 2006). In addition, whereas ICF augmentation was small, SICI decreased gradually and disappeared 60 ms before voluntary EMG (Nikolova *et al.*, 2006). Reynolds and Ashby (1999) reported that the increase of MEP in response to single pulse TMS and the decrease of SICI were significant before the onset of voluntary movement, while the decrease of SICI appeared in advance of the increase of MEP by single pulse TMS. Alegre *et al.* (2003) also demonstrated that a decrease in beta band EEG activity began contralaterally approximately 1.5 s prior to the onset of movement, and that the decrease began in the alpha band at 1 s before the movement. These results suggest that ERD during motor imagery may induce changes in cortical excitability, which is similar to the changes accompanying actual movements and their anticipation.

2.4.2 Frequency Components of Event-Related Desynchronization Representing Cortical Excitability

Many previous studies have demonstrated that a decrease in sensorimotor EEG power reflects corticospinal excitability, but the effective frequency band representing corticospinal excitability remains unclear. One study demonstrated a positive correlation between MEP amplitude and alpha ERD induced by repetitive hand movement (Hummel *et al.*, 2002), though MEP amplitude was also correlated with beta ERD induced by brisk hand movement (Schulz *et al.*, 2013). Negative correlations between MEP amplitude and sensorimotor EEG power in either alpha (Sauseng *et al.*, 2009) or beta bands (Mäki and Ilmoniemi, 2010) were also found at rest. Thus, such conflicting results were assumed to be attributed to movement

type, experimental settings, and/or differences in data analysis (Schulz *et al*., 2013).

In the present study, SICI of FCR muscle was positively correlated with averaged ERD in the frequency band displaying the largest ERD during motor imagery, but not in alpha or beta band. SICI of ECR muscle was correlated with averaged ERD in the both frequency band displaying the largest ERD and alpha and beta bands, and the correlation between ERD and SICI of ECR muscle was tended to be higher in the frequency range displaying the largest ERD compared to alpha and beta bands. The frequency band displaying the largest ERD was different for each participant even though the motor type, experimental settings, and analysis method were invariable between participants. This indicates the ERD frequency band representing cortical excitability differs between individuals. Moreover, the present results suggested that the discrepancy in previous findings might be caused by inter-subject variability of the frequency band representing neural excitability.

2.4.3 Muscle Dependency and Motor Imagery Task

In the present study, the participants were asked to perform either motor imagery of wrist flexion or extension, and EMG was recorded from the agonist (FCR or ECR) muscle of the imagined movement. As a result, SICI of ECR muscle was correlated with not only ERD in the frequency band displaying the largest ERD in the screening session but also the alpha and beta ERD, whereas SICI of FCR muscle was solely correlated with ERD in the frequency band displaying the largest ERD (Fig. 2-5). These results indicate that both motor imagery of wrist flexion and extension accompanied by ERD can modulate the M1 excitability but their effects are not fully consistent.

The difference in the effect of the motor imagery task on the M1 excitability may lie in the limb posture. In the present study, participants were asked to put their hand on the

table with palm side down. This limb posture enables participants to extend their wrist, but not to flex their wrist. Vargas *et al*. (2004) demonstrated that the limb posture compatible with the motor imagery task induced a higher increase in the MEP amplitude during motor imagery when compared with an incompatible posture. Therefore, it is highly possible that the actual limb posture affects the process of motor imagery, resulting in a difference in the M1 excitability level represented by an ERD.

The M1 excitability during motor imagery would be influenced by the anatomical property of the agonist muscle of imagined movement. Histological research in non-human primates found that corticomotoneuronal cells of the wrist extensor have a larger muscle field than the flexor corticomotoneuronal cells (Fetz and Cheney, 1980; Kasser and Cheney, 1985). In consistent with this finding, the degree of facilitation during agonist muscle contraction was greater for the ECR muscle than for the FCR muscle in humans (Chye *et al*., 2010). However, other evidence also from humans demonstrated the degree of facilitation during agonist muscle contraction was greater for the FCR muscle than for the ECR muscle (Izumi *et al*., 2000). Hashimoto and Rothwell (1999) reported that the TMS-evoked descending volley to the FCR muscle was facilitated during the period of imagined movement of wrist flexion, and that the size of the descending volley to the ECR muscle was similarly facilitated during the period of imagined movement of wrist extension. Although the differences in the characteristics of the FCR and ECR muscles remain unclear, the present results extend previous work by showing that ERD during motor imagery of wrist movement reflects the M1 excitability of agonist muscles regardless of whether flexor or extensor.

Chapter 3

Event-Related Desynchronization Represents the Excitability of Human Spinal Motoneurons

3.1 Introduction

Several distinct cortical circuits, such as the basal ganglia-thalamocortical circuit and the parietal-premotor circuit, contribute to voluntary movements (Haggard, 2008). These circuits converge on the M1, which conveys motor commands to spinal motoneurons and muscles. The cortical activity accompanying voluntary movements is often investigated by EEG, in which waveforms reflect the electric activity of cortical neurons.

ERD is one of the motor-related EEG components and is observed over the contralateral sensorimotor area as well as several higher motor cortices (such as the SMA and posterior association cortex) during movement preparation (Babiloni *et al*., 1999). Movement preparation corresponds to a subliminal activation of the motor cortical system, with a similar mechanism underlying motor imagery (Sohn *et al*., 2003). The research presented in Chapter 2 extended previous work by showing that ERD, during motor imagery, related to the M1 excitability of the agonist muscles regardless of whether they are flexor or extensor. This finding leads to a further question whether increased motor cortical excitability associated with an ERD during motor imagery influences spinal excitability.

Voluntary relaxation depresses spinal motoneurons, whereas motor imagery without overt muscle contraction counters this effect (Fujisawa *et al*., 2011; Hara *et al*., 2010; Ichikawa *et al*., 2009; Taniguchi *et al*., 2008). Mercuri *et al*. (1996) demonstrated a transient

facilitation of spinal motoneurons by subthreshold TMS to the M1. Long-term potentiation-like plasticity in the M1, induced by subthreshold 5-Hz repetitive TMS, increases spinal excitability (Quartarone *et al*., 2005). These studies inferred that the leaked cortical volley elicited by the motor imagery involving ERD might facilitate spinal motoneurons without overt muscle contractions. Nevertheless, no empirical evidence is available concerning the correlation between motor-related EEG components and spinal motoneuronal excitability.

The purpose of the present study was to assess the association between ERD in scalp EEG and the excitability of spinal motoneurons during motor imagery. For testing spinal motoneuronal excitability at a fixed ERD magnitude, the median nerve was stimulated on the first instance the sensorimotor ERD exceeded the predetermined threshold during hand motor imagery. F-wave was recorded from the intrinsic hand muscle, and F-wave measurements for different ERD magnitudes were examined. The difference in the ERD topography during motor imagery was also compared between trials in which the apparent F-wave was either confirmed (the condition of higher spinal excitability) or not confirmed (the condition of lower spinal excitability). It may clarify the contribution of the activity of both the M1 and non-M1 regions on the excitability of spinal motoneurons.

3.2 Materials and Methods

3.2.1 Participants

Fifteen healthy participants (aged 22.1 ± 1.7 years; 12 males, 3 females) joined this study. All were right-handed, without any medical or psychological disorders, and had normal vision (according to self-reports). All participants were initially naïve to the experiment. The purpose and experimental procedure were explained to the participants and written

informed consent was obtained. The study was approved by the local ethics committee of Keio University (#24-23) and performed in accordance with the Declaration of Helsinki.

3.2.2 Data Acquisition

EEG was recorded with 23 g.LADYbird active electrodes in g.GAMMA cap^2 (g.tec medical engineering GmbH, Graz, Austria). Electrodes were placed at Fp1, Fp2, F7, F3, Fz, F4, F8, FC3, T3, C5, C3, C1, Cz, C4, T4, CP3, T5, P3, Pz, P4, T6, O1, and O2, as designated according to the International 10–20 System. The ground electrode was located on the forehead, and the reference electrodes mounted on both right and left earlobes. EEG signals were band-pass filtered (0.1–100 Hz with 4th order Butterworth) with a notch (50 Hz for avoiding power line contamination) and digitized at 512 Hz using a biosignal amplifier (g.USBamp; g.tec medical engineering GmbH).

The F-wave, which is an orthodromically evoked CMAP, was recorded from the right abductor pollicis brevis (APB) muscle using bipolar Ag/AgCl electrodes of 10 mm in diameter. The cathode was placed over the belly of the APB muscle, and the anode was placed over the tendon near the metacarpophalangeal joint of the thumb. Impedance for all channels was maintained below 20 kΩ throughout the experiment. F-wave signals were band-pass filtered (20 Hz–2 kHz with 2nd order Butterworth), digitized at 10 kHz using a biosignal amplifier (Neuropack MEB-9200; Nihon Kohden, Tokyo, Japan), and monitored throughout the experiment.

To elicit F-waves, the stimulating electrodes consisted of the cathode, which was placed over the right median nerve 3 cm proximal to the palmar crease of the wrist joint, and the anode, which was 2 cm proximal to the cathode (Fujisawa *et al*., 2011). The stimulus was determined by delivering 0.2 ms square-wave pulses with increasing intensity to elicit the

maximal M-wave. Supramaximal shocks, 20% higher than the stimulus intensity to elicit the maximal M-wave, were delivered for acquiring F-waves with the fixed repetitive time schema as described below (*3.2.3 Experimental Protocol*). The recording of each F-wave began 50 ms prior to median nerve stimulation and ended after 100 ms.

3.2.3 Experimental Protocol

Each participant took part in a series of four experimental sessions: Screening session and F-wave Conditions 1, 2, and 3. Initially, each participant engaged in the screening session. Following this, participants performed F-wave Conditions 1, 2, and 3, which were randomly determined so that the order was different for each participant. The screening session and F-wave Conditions 1, 2, and 3 were performed on the same day.

In the screening session (Fig. 3-1a), the participant sat in a comfortable armchair and placed their palm upward on the armrest. A 24-inch computer monitor was placed 1 m in front of the participant's eyes. The screening session consisted of 30 trials. Each trial started with the presentation of the word 'Rest' at the center of the monitor. Six seconds later, the word 'Ready' was presented for 1 s. The monitor then displayed the word 'Execution' and the participant performed sustained thumb abduction for 5 s. After a short pause, the monitor displayed the word 'Rest', and the next trial began.

In F-wave Condition 1 (Fig. 3-1a), I applied suprathreshold electrical stimulation to the right median nerve at the wrist level during the rest condition. Background EMG activity was monitored during the experiment, and trials contaminated by more than ±20 μV of background EMG activity were discarded. Electrical stimulation was applied at least fifty times at intervals of 12.0 ± 5.0 s, and fifty CMAPs without any background EMG activity were collected.

F-wave Condition 2 (Fig. 3-1a) was conducted using the same time scheme as the screening session, but the participants performed kinesthetic motor imagery of sustained thumb abduction for 5 s instead of performing the actual movement. In addition, the monitor did not show any words during motor imagery. Participants received visual feedback of ERD magnitude in the form of a continuously moving bar displayed on the monitor during the 5-s motor imagery period. Participants were informed successful hand motor imagery would shift the bar to the right edge of the monitor and unsuccessful hand motor imagery would shift the bar to the left edge. I applied suprathreshold electrical stimulation to the right median nerve at the wrist level on the first instance the ERD during the hand motor imagery exceeded 5% (Fig. 3-1b). The background EMG activity was monitored during the experiment and trials contaminated by more than ±20 μV of background EMG activity were discarded. Electrical stimulation was applied at least fifty times and fifty CMAPs were collected. F-wave Condition 3 was performed using the same conditions as F-wave Condition 2. However, in this condition, nerve electrical stimulation was applied immediately after ERD during motor imagery exceeded 15%.

I applied median nerve stimulation 50 times with an inter-stimulus interval of 9.5 ± 2.5 s in F-wave Condition 1, and at a certain ERD magnitude during hand motor imagery in F-wave Conditions 2 and 3. My protocol requires placing the stimulating electrode on the wrist for an extended period in comparison with the general median nerve stimulation protocol (100 times at 1 Hz). The stimulating electrode was repositioned to the most stable area for F-wave evocation at the beginning of each F-wave Condition to minimize the risk of the stimulating electrode deviating from its best position. The experiment was halted if any F-wave Condition exceeded 15 minutes. The stimulating electrode was then repositioned to an optimal point for F-wave evocation and the rest of the trials were

resumed. I confirmed the stimulus intensity to elicit the maximal M-wave did not change before and after any rearrangement.

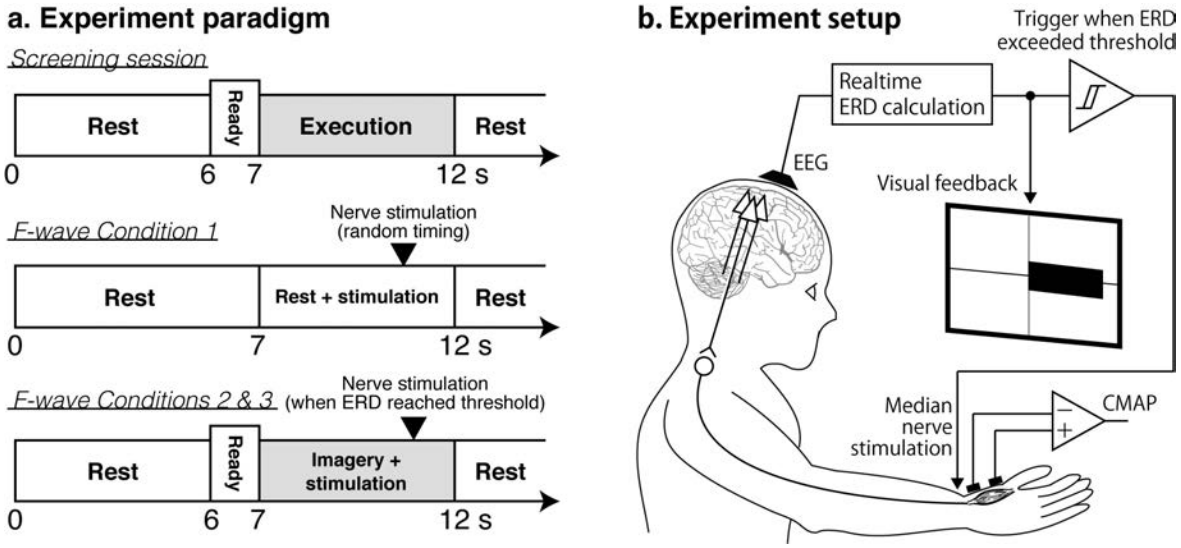

Figure 3-1. Experimental setup and paradigm

(a) Experimental paradigm of the screening session, and F-wave Conditions 1, 2, and 3. (b) Experimental system for the F-wave Conditions 2 and 3.

3.2.4 F-wave Analysis

First, I visually classified CMAPs depending on whether F-wave responses were observed or not. An average of the CMAPs with no F-wave responses was used for the baseline, and baseline-subtracted peak-to-peak amplitude of CMAPs was measured between 21 and 40 ms after median nerve stimulation. I defined a peak-to-peak amplitude larger than 50 μV as an 'apparent F-wave response' and that smaller than 50 μV as an 'absent F-wave response'. It is difficult to distinguish evoked EMG responses with a peak-to-peak amplitude of less than 50 μV from noise (Rossini *et al.*, 1994). F-wave measurements consisted of persistence (defined as the percentage number of apparent F-wave responses per 50 stimuli), onset latency, and

peak-to-peak amplitude averaged in two ways: (1) counting all trials (50) including absent F-wave responses as 0 μV (trial average) and (2) counting only those trials with apparent F-wave responses (response average).

3.2.5 Electroencephalogram Analysis

Detailed methods of online ERD calculation and the visual feedback of ERD magnitude are reported in the previous chapter (*2.2.4 Electroencephalogram Analysis*). Here I briefly described the online and the offline algorithm for calculating ERD.

ERD was defined as a decrease in the EEG power spectrum compared with a baseline period, defined as the interval from -3 s to the time 'Ready' was displayed on the monitor. ERD was calculated with a time resolution of 62.5 ms and a frequency resolution of 1 Hz during each 5-s task period. I then determined the best electrode setup and frequency band within alpha and beta bands in the screening session with each participant. Pairs of C3 and FC3, CP3, C5, and C1 bipolar EEG signals were used to define the electrode pair and the 3 Hz width frequency band displaying the largest ERD. The electrode pair and the frequency band displaying the largest ERD were used for online ERD calculations in F-wave Conditions 2 and 3.

I also performed offline ERD analysis using 19 channels of the EEG signals (excluding FC3, C5, C1, and CP3), which were re-referenced by a four neighbors Laplacian spatial filter (Hjorth, 1975). All EEG signals were visually controlled for artifacts and discarded in cases of artifact-contaminated trials. ERD was then calculated from a 1-s EEG epoch prior to the nerve stimulation compared with the baseline period. Since F-wave Condition 1 was a resting condition, I used the interval from 3 to 6 s of each trial as the baseline period of F-wave Condition 1. Baseline period of F-wave Conditions 2

and 3 were the same interval as the online analysis. Spatially interpolated topographic ERD maps were plotted in accordance with their channel locations over the scalp using trial average of ERD magnitudes just prior to the nerve stimulation. Both ERD and F-wave analysis were performed using MATLAB 2010b (MathWorks, Natick, MA).

3.2.6 Statistical Tests

One-way ANOVA with repeated measures was used to determine the effect of experimental conditions on F-wave measurements (persistence, onset latency, trial average, and response average of the F-wave amplitude), frequency of nerve stimulation, and averaged EEG power values for the baseline period, which was calculated with the bipolar channel and the frequency band displaying largest ERD as shown in Table 3-1. In addition, to verify the spatial configuration of ERD during hand motor imagery, ERD magnitude in the frequency band displaying largest ERD, which was calculated with 1-s Laplacian EEG data prior to the nerve stimulation, was compared among experimental conditions and brain regions (i.e., EEG channels) using two-way ANOVA with repeated measures. If ANOVA yielded a significant F value, Tukey's post-hoc test was performed. Type I error was set to 0.05. Statistical test was performed using SPSS ver. 21.0 (SPSS Inc., Chicago, IL).

3.3 Results

3.3.1 F-wave Measurements

Figure 3-2a illustrates a typical example of M- and F-wave traces recorded from APB muscle in all experimental conditions. Figure 3-3 represents individual and mean values for F-wave persistence, trial and response averages of F-wave amplitude in the resting condition, and during motor imagery of right thumb abduction at ERD 5% and 15%. F-wave persistence was 38 ± 14% in the resting condition, 46 ± 15% in the motor imagery at ERD 5%, and 58 ± 20% in the motor imagery at ERD 15% ($F_{2, 28}$ = 20.7, P < .001). The persistence was significantly higher at ERD 5% (P < .05) and 15% (P < .001) when compared with the resting condition, and higher at ERD 15% when compared with ERD 5% (P < .01). The trial amplitude average was 56.8 ± 39.5 μV in the resting condition, 81.6 ± 51.4 μV in the motor imagery at ERD 5%, and 101.2 ± 56.2 μV in the motor imagery at ERD 15% ($F_{2, 28}$ = 8.17, P < .01). This was significantly larger at ERD 15% (P < .01) when compared with the resting condition. The response amplitude average was not different between experimental conditions [rest = 136.7 ± 60.3 μV, motor imagery at ERD 5% = 163.8 ± 66.6 μV, motor imagery at ERD 15% = 163.1 ± 64.4 μV ($F_{2, 28}$ = 2.48, P > .05)].

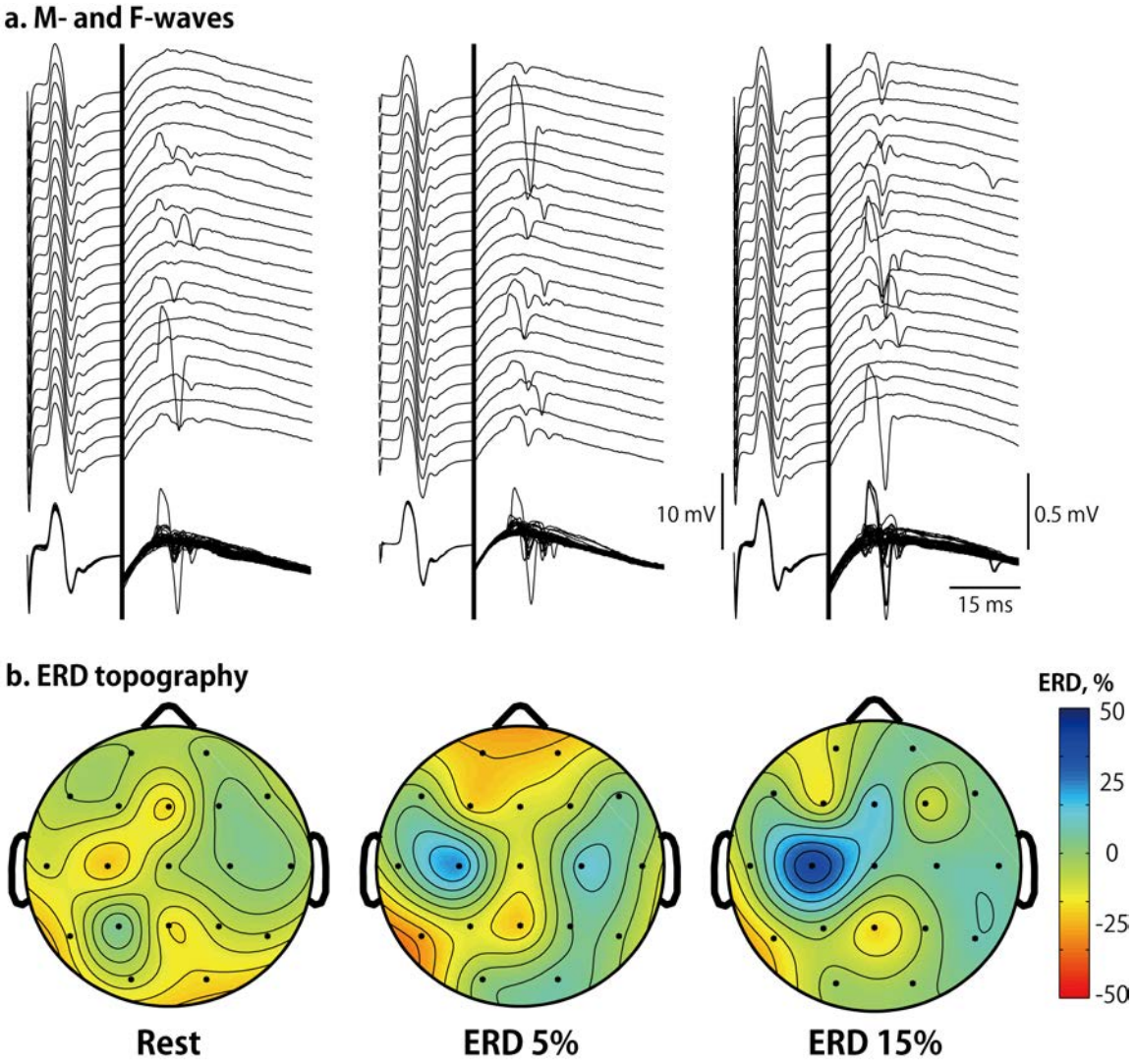

Figure 3-2. M- and F-wave traces and ERD topographies in one representative participant (Participant 1A)

(a) Upper traces were 20 consecutive M- and F-waves. Lower traces were 50 consecutive M- and F-waves overlaid per condition. These CMAPs were recorded from APB muscles during the resting condition and hand motor imagery at ERD 5% and 15%. As the ERD increased, F-wave persistence was markedly increased. (b) ERD topographies were reconstructed from 19-channel EEG data in the frequency range of 12–14 Hz, which was the most reactive frequency band displaying ERD of participant 1A. Electrode positions are shown by dots. Positive values (blue colors) indicate strong ERD.

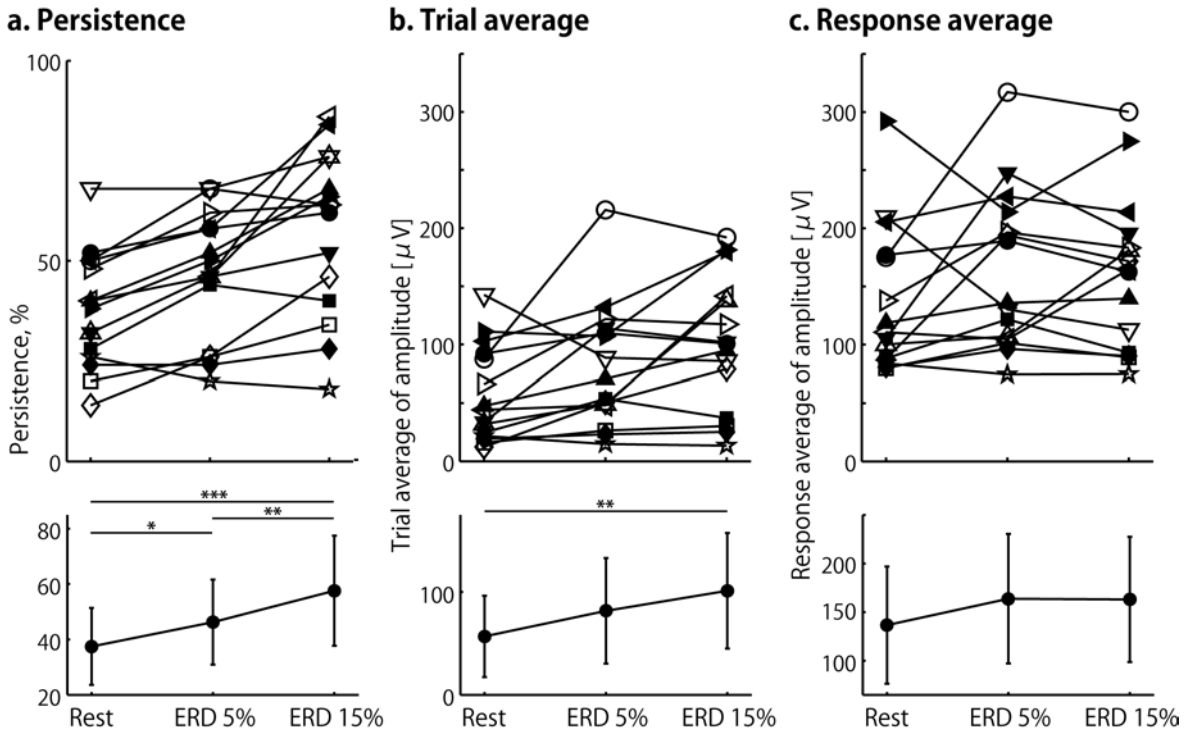

Figure 3-3. F-wave measurements in the resting condition and during hand motor imagery at ERD 5% and 15%

(a) F-wave persistence, (b) trial average, and (c) response average of F-wave amplitude. Upper panels: each line shows the result obtained from each participant (N = 15). Lower panels: mean values. Error bar indicates standard deviation. * P < .05, ** P < .01, *** P < .001.

The effect of ERD on onset latency was not significant [rest = 26.0 ± 1.02 ms, motor imagery at ERD 5% = 26.3 ± 1.29 ms, motor imagery at ERD 15% = 26.3 ± 1.13 ms ($F_{2, 28}$ = 0.95, P > .05)], though the mean interval of the nerve stimulation was significantly different between the experimental conditions [rest = 12.0 ± 0.00 s, motor imagery at ERD 5% = 13.7 ± 1.25 s, motor imagery at ERD 15% = 15.1 ± 4.74 s ($F_{2, 28}$ = 19.8, P < .001)]. Post-hoc test revealed the mean stimulus interval was significantly lower at ERD 5% (P < .001) and 15% (P < .001) compared with the resting condition. The results of F-wave

measurements were summarized into Table 3-1.

Table 3-1. F-wave measurements in the resting condition, and during right hand motor imagery at ERD 5% and ERD 15%

Persistence, %	Rest	38 ± 14
	ERD 5%	46 ± 15
	ERD 15%	58 ± 20
Trial average [μV]	Rest	56.8 ± 39.5
	ERD 5%	81.6 ± 51.4
	ERD 15%	101.2 ± 56.2
Response average [μV]	Rest	136.7 ± 60.3
	ERD 5%	163.8 ± 66.6
	ERD 15%	163.1 ± 64.4
Latency [ms]	Rest	26.0 ± 1.02
	ERD 5%	26.3 ± 1.29
	ERD 15%	26.3 ± 1.13
Stimulus interval [s]	Rest	12.0 ± 0.00
	ERD 5%	13.7 ± 1.25
	ERD 15%	15.1 ± 4.74

Values represent mean ± SD.

I tested whether the number of apparent F-wave responses was related to the trial number for the motor imagery task. The number of apparent F-wave responses in the ERD 5% condition were 5 ± 2, 4 ± 2, 5 ± 2, 4 ± 2, and 5 ± 2 in trial numbers 1–10, 11–20, 21–30, 31–40, and 41–50, respectively. In the ERD 15% condition, the number of apparent F-wave responses were 6 ± 2, 4 ± 2, 6 ± 2, 7 ± 2, 5 ± 2 in trial numbers 1–10, 11–20, 21–30, 31–40, and 41–50, respectively. One-way repeated measures ANOVA found no

significant relationship between the number of apparent F-waves and trial number of motor imagery task in the both ERD 5% ($F_{4, 56}$ = 0.48, P > .05) and ERD 15% conditions ($F_{4, 56}$ = 2.29, P > .05).

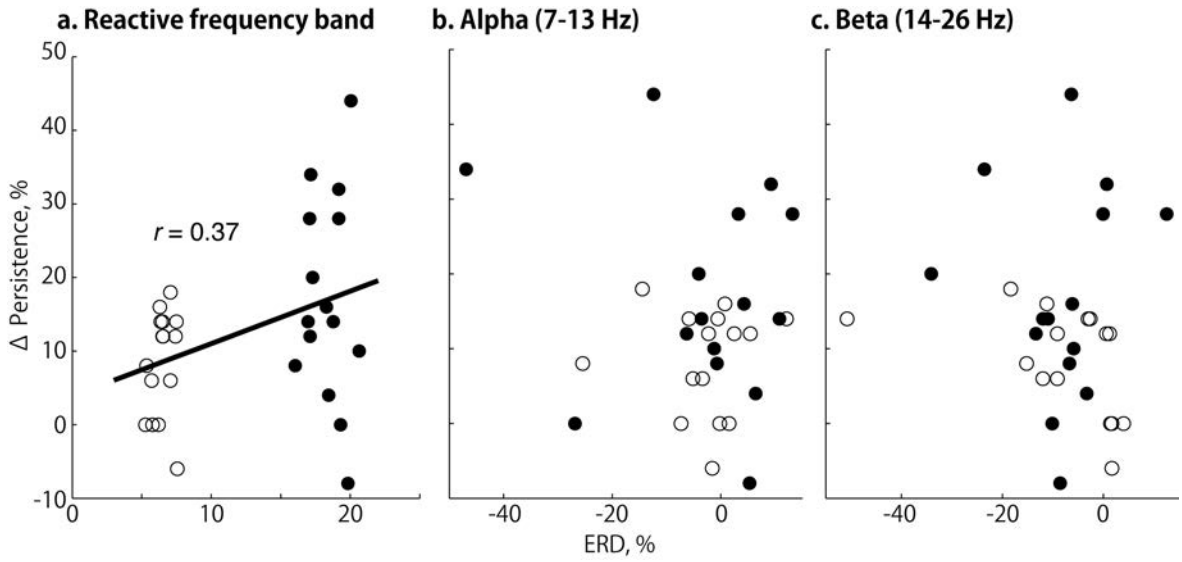

Figure 3-4. Relationship between ERD frequency band and F-wave persistence

X-axis represents averaged ERD value calculated with 1-s bipolar EEG data prior to the nerve stimulation, in the frequency range of the most reactive frequency band displaying ERD in the screening session (a), 7–13 Hz (b), and 14–26 Hz (c). Positive values indicate strong ERD. Y-axis represents subtraction of F-wave persistence in F-wave Conditions 2 and 3 from F-wave Condition 1. Open and filled circles reflect data from F-wave Conditions 2 and 3, respectively.

Correlations between F-wave persistence and ERD values in different frequency ranges (i.e., alpha, beta, and the most reactive frequency band displaying ERD in the screening session) were also compared (Fig. 3-4). ERD was calculated with 1-s EEG data prior to the nerve stimulation derived from the electrode pair displaying the largest ERD in the

screening session. Results showed F-wave persistence was significantly correlated with averaged ERD in the most reactive frequency band displaying ERD (Fig. 3-4a; $r_{28} = 0.37$, $P < .05$), but not with alpha (Fig. 3-4b) or beta (Fig. 3-4c) ERD.

3.3.2 Spectral Power of Electroencephalogram

In the screening session, all participants showed ERD around the C3 channel during right thumb movement. The characteristics of the ERD, such as the most reactive frequency band and bipolar channel in the screening session, are summarized in Table 3-2.

Table 3-2. Frequency band and bipolar channel displaying the largest ERD during right thumb abduction in the screening session

Participant	Channel	Frequency [Hz]
2A	C3-C1	12–14
2B	C3-CP3	12–14
2C	C3-C1	11–13
2D	C3-FC3	11–13
2E	C3-C1	16–18
2F	C3-FC3	13–15
2G	C3-C1	12–14
2H	C3-CP3	10–12
2I	C3-C1	13–15
2J	C3-FC3	7–9
2K	C3-FC3	10–12
2L	C3-FC3	11–13
2M	C3-C1	10–12
2N	C3-FC3	16–18
2O	C3-FC3	10–12

I found no significant differences in the bipolar EEG power values during the baseline period between F-wave Conditions 1, 2, or 3 ($F_{2, 28} = 0.53$, $P > .05$). This indicates there are similar mean baseline power values for the resting and motor imagery conditions.

Figure 3-2b represents a typical example of ERD topographic maps in F-wave Conditions 1, 2, and 3 from the 19-channel EEG signals. The maps were constructed from averaged ERD values calculated from 1-s Laplacian EEG data prior to nerve stimulation in a frequency range of 12–14 Hz, which was the most reactive frequency band displaying ERD in the screening session. For all participants, significant main effects for experimental conditions ($F_{2, 28} = 14.7$, $P < .001$) and EEG channels ($F_{18, 252} = 3.01$, $P < .001$) were found. Post-hoc tests revealed the ERD magnitude at C3 was significantly larger than the ERD magnitude at channels FP1, FP2, F7, Fz, F4, F8, T7, Cz, C4, T8, and P7 in F-wave Condition 2. It was also larger than the ERD magnitude at all EEG channels except P3 in F-wave Condition 3 ($P < .05$). No significant differences were observed in F-wave Condition 1. The strongest ERD was observed at C3 in F-wave Conditions 2 and 3. This suggests the observed ERD during right hand motor imagery mainly localized to the contralateral sensorimotor area in this experimental procedure.

To confirm the effect of cortical activity in non-M1 regions on spinal excitability during hand motor imagery, the difference of the ERD topography between the apparent F-wave trials and non F-wave trials was compared. ERD values were calculated from 1-s Laplacian EEG data prior to nerve stimulation in F-wave Conditions 2 and 3. The ERD values were then classified into two groups: trials with F-wave $\geq$ 50 μV (apparent F-wave trials) and trials with F-wave < 50 μV (non F-wave trials). The maps were constructed from the averaged ERD values across the trials in the most reactive frequency band displaying ERD of each participant (Fig. 3-5). The ERD value of each electrode in the apparent F-wave

trials and non F-wave trials were statistically compared using the unpaired t-test with Bonferroni correction. The results showed that ERD was significantly larger in the apparent F-wave trials compared to the non F-wave trials at EEG channels of Cz ($P < .05$), C3 ($P < .05$), and P3 ($P < .05$). The results are summarized in Table 3-3.

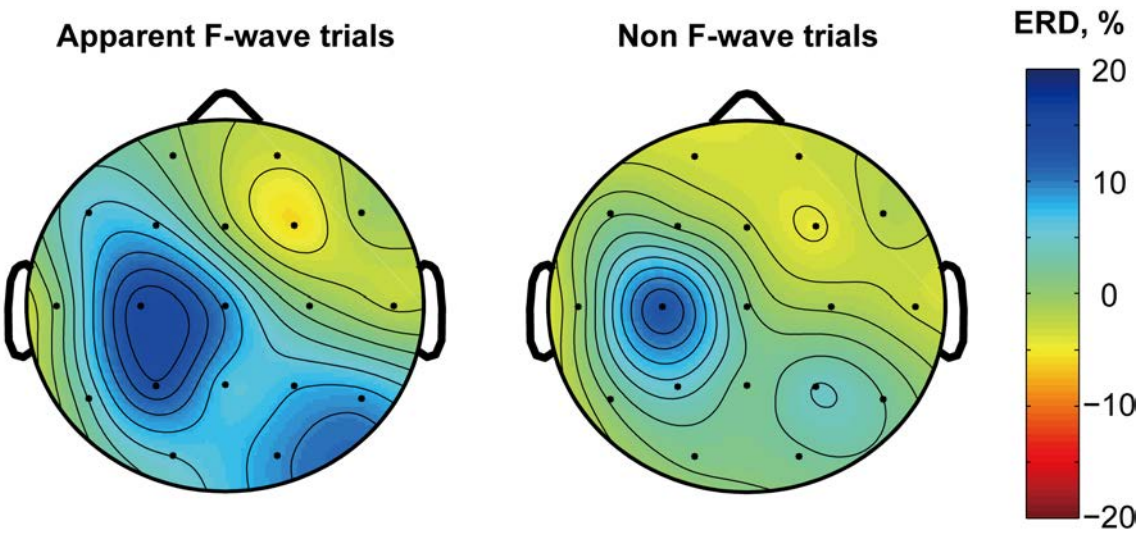

Figure 3-5. ERD topographies on the apparent and non F-wave trials during hand motor imagery

ERD values were calculated using 1-s Laplacian EEG data prior to nerve stimulation in the most reactive frequency band displaying ERD of each participant. The left and right topography maps represent the averaged ERD of the apparent and non F-wave trials, respectively. Electrode positions are shown by dots. Positive values (blue colors) indicate strong ERD.

Table 3-3. EEG channels with significant difference in ERD values between apparent and non F-wave trials

		ERD, %
Cz	Apparent F-wave trials	10.3 ± 34.9
	Non F-wave trials	1.6 ± 33.1
C3	Apparent F-wave trials	15.3 ± 12.3
	Non F-wave trials	12.6 ± 10.9
P3	Apparent F-wave trials	13.3 ± 34.0
	Non F-wave trials	5.1 ± 32.4

Values represent mean ± S.D.

3.3.3 Effects of Task Compliance on the Spinal Excitability

The relationship between F-wave persistence, an index of the spinal motoneuronal excitability, and the task success rate, an index of task difficulty, was examined. Task success was defined as when the EEG power in a certain frequency band decreased 5% or 15%, relative to the baseline period, during the 5-s motor imagery period in F-wave Conditions 2 and 3, respectively. The percentage of task success in F-wave Conditions 2 and 3 were 83 ± 10% and 75 ± 12%, respectively. This difference was statistically significant (t_{14} = 2.93, P < .05), but the correlation between F-wave persistence and percentage of task success was not significant (Fig. 3-6a; P > .05). I also compared the duration of hand motor imagery before nerve stimulation in F-wave Conditions 2 and 3. The result was 1.0 ± 0.2 s in F-wave Condition 2 and 1.6 ± 0.3 s in F-wave Condition 3, the difference being statistically significant (t_{14} = 9.22, P < .001). However, there was no significant correlation between F-wave persistence and the time duration of hand motor imagery (Fig. 3-6b; P > .05).

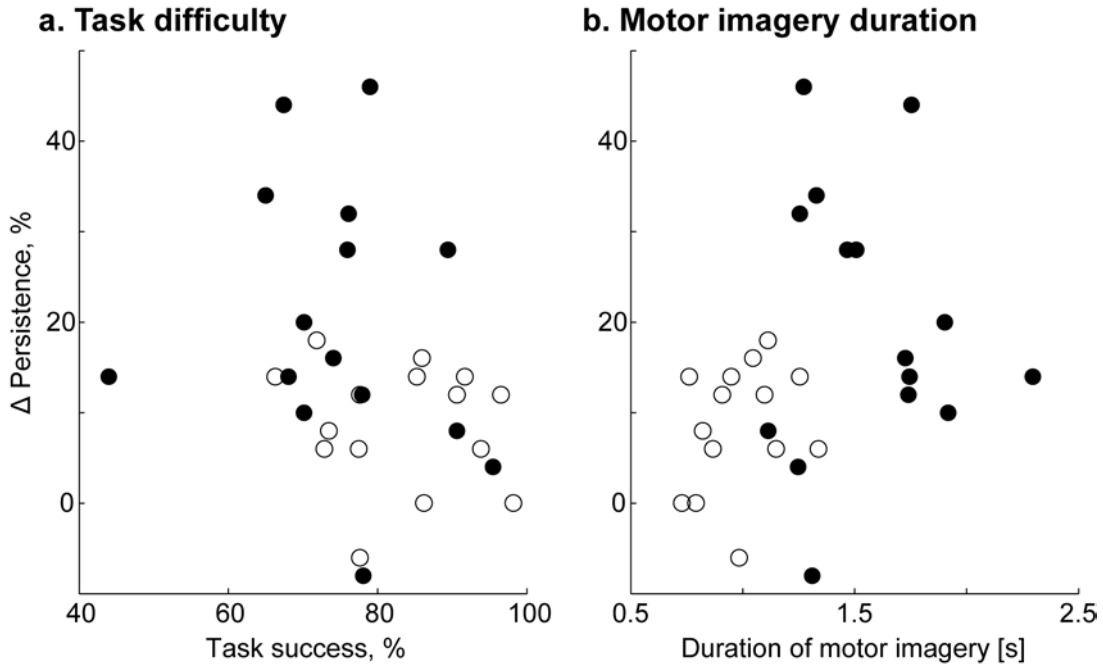

Figure 3-6. Correlation between F-wave persistence, (a) percentage of task success, and (b) duration of motor imagery before nerve stimulation

Y-axis represents subtraction of the F-wave persistence in F-wave Conditions 2 and 3 from F-wave Condition 1. Open and filled circles reflect data from F-wave Conditions 2 and 3, respectively.

3.4 Discussion

3.4.1 Relationship between Sensorimotor Event-Related Desynchronization and the Spinal Excitability

I found ERD magnitude during hand motor imagery was associated with a significant increase in F-wave persistence and the trial average of F-wave amplitude, but no significant changes were found in the response average of F-wave amplitude or F-wave latency. Rivner (2008) suggested that the response average of F-wave amplitude, which regards only apparent F-wave responses, relates to the type of motoneuron excited rather than the general spinal excitability. This means an increase in the response average of F-wave amplitude would indicate a shift in motor units recruited from smaller to larger ones. By contrast, F-wave persistence, which is the percentage number of apparent F-wave responses for all stimuli, is probably best considered a measure of increased spinal motoneuronal excitability. The trial average of F-wave amplitude, which counts absent F-wave responses as 0 μV, would be influenced by the excitability of total spinal motoneurons. F-wave latency is influenced by the conduction velocity of recruited motoneurons, but is unlikely to be influenced by corticospinal activity (Fujisawa *et al*., 2011; Hara *et al*., 2010; Ichikawa *et al*., 2009; Taniguchi *et al*., 2008). The present study indicates ERD magnitude during hand motor imagery represents an increase in the general excitability of the spinal motoneurons, but does not reflect the type of excited motoneurons or the conduction velocity of the recruited motoneurons.

The study presented in Chapter 2 demonstrated that intracortical excitability was strongly correlated with ERD values in the frequency range displaying the largest ERD during motor imagery compared to the alpha and beta bands. I argued that ERD frequency band representing cortical excitability might differ between individuals. Herein, F-wave

persistence positively correlated with the averaged ERD in the frequency band displaying the largest ERD during the actual hand movement, but not in the alpha or beta bands. The frequency band displaying the largest ERD was different for each participant even though the motor type, experimental settings, and analysis method were invariable between participants. Thus, the present results suggested that the ERD frequency band representing the excitabilities of both the M1 and spinal motoneurons differs between individuals.

Why does ERD magnitude during hand motor imagery reflect the excitability of spinal motoneurons? ERD magnitude is related to the MEP amplitude (Hummel *et al*., 2002; Mäki and Ilmoniemi, 2010; Sauseng *et al*., 2009; Shultz *et al*., 2013). This implies larger ERD induces greater M1 activation at least. Thus, an increase in M1 excitability accompanying motor imagery tasks involving ERD might enhance subthreshold activation of spinal motoneurons because these motoneurons have monosynaptic corticomotoneuronal connections, particularly to finger muscles (Lemon *et al*., 2004). Mercuri *et al*. (1996) demonstrated facilitation of the F-wave by subthreshold TMS to the M1. They also emphasized the very transient nature of spinal excitability changes, which return to baseline values unless the corticospinal descending volley evoked by subthreshold TMS collides with the antidromic volley induced by supramaximal median nerve stimulation. On the other hand, the precise timing of the central drive would be unnecessary for increasing spinal excitability. Quartarone *et al*. (2005) showed a sustained increase of spinal excitability after subthreshold 5-Hz repetitive TMS to the M1, which is a known method to increase corticospinal excitability (Pascual-Leone *et al*., 1994). Thus, I still do not know whether a motor imagery task increases the excitability of spinal motoneurons transiently or sustainably, even though no significant relationship between the number of apparent F-waves and the trial number of the motor imagery task would suggest that the ERD magnitude during hand motor imagery

represents transient excitability of the spinal motoneurons.

I noted here that the averaged interval of the nerve stimulation was significantly lower at ERD 5% and 15% conditions compared with the resting condition. One concern is that F-wave persistence was influenced by the stimulus interval rather than an increase in spinal excitability. However, whereas Fierro *et al*. (1991) reported that the interval of the nerve stimulation was negatively correlated with both F-wave persistence and amplitude, the present results showed a positive correlation between the F-wave persistence and the stimulus interval. Additionally, F-wave persistence and amplitude in the present study seem to be too small when compared with those in the literature generally. The persistence of APB muscle typically ranges from 60-70% and the response amplitude ranges from 150-200 μV with a stimulus frequency of 1 Hz (Fujisawa *et al*., 2011; Ichikawa *et al*., 2009; Taniguchi *et al*., 2008). I considered that the low F-wave persistence and amplitude was caused by the long stimulus interval. The present F-wave measurements therefore reflect the excitability of spinal motoneurons per se. Moreover, F-wave persistence in the motor imagery task was not correlated with time to exceed the predetermined threshold or task success percentage. These results suggest an increase in spinal excitability was associated with ERD magnitude during hand motor imagery, but not with the duration of motor imagery and task difficulty.

3.4.2 Association of the Topography of Event-Related Desynchronization with Spinal Excitability

Comparing ERD topography of the apparent F-wave trials (a condition of higher spinal excitability) with non F-wave trials (a condition of lower spinal excitability), ERD at EEG channels of Cz, C3, and P3 was significantly larger in the apparent F-wave trials. The position of C3 corresponds to the hand sensorimotor area, Cz partially overlaps with the

SMA, and P3 is close to the inferior parietal lobe, a part of the parietal association cortex (Herwig *et al*., 2003). The ERD topography of the apparent F-wave trials was similar to the ERD topography during the voluntary hand movement shown by using high-density scalp EEG (Babiloni *et al*., 1999) and electrocorticogram (Pfurtscheller *et al*., 2003). They illustrated that ERD was observed over the contralateral sensorimotor area as well as the SMA and parietal association cortex during the voluntary hand movement. Therefore, the present result implied that the necessity to induce brain activity state is similar to the actual movement for increasing spinal excitability accompanying motor imagery. One concern of this discussion is that EEG signals of Cz and P3 can be influenced by the activity of both the primary sensorimotor and higher motor cortices, because scalp EEG is a spatiotemporally smoothed version of the local field potential. Future study, in which spinal motoneuronal excitability is tested during hand motor imagery with suppressed activity of the higher motor cortices, e.g., applying 1 Hz repetitive TMS to the SMA (Neubert *et al*., 2010), will provide insight about the contribution of the activation of the higher motor cortices to the increase in spinal excitability.

3.4.3 Comparison of F-wave and H-reflex Responses

The present results demonstrated a facilitatory effect of hand motor imagery on the F-wave, as several authors have documented (Fujisawa *et al*., 2011; Hara *et al*., 2010; Ichikawa *et al*., 2009; Rossini *et al*., 1999; Taniguchi *et al*., 2008). However, others have reported MEP enhancement without significant changes in simultaneously recorded F-wave during hand motor imagery (Facchini *et al*., 2002; Patuzzo *et al*., 2003; Sohn *et al*., 2003; Stinear *et al*., 2006). These previous studies, which found no effect of hand motor imagery on F-wave, applied less than 25 nerve stimuli, whereas ≥50 stimuli are needed to obtain accurate

F-wave measurements reflecting spinal motoneuronal excitability (Lin and Floeter, 2004). Because 50 stimuli were applied in the present study, the present F-wave measurements are considered to reflect the actual excitability of spinal motoneurons.

The present results are also different from those obtained using the H-reflex technique (Abbruzzese *et al*., 1996; Hashimoto and Rothwell, 1999; Kasai *et al*., 1997; Patuzzo *et al*., 2003), which showed no facilitatory effect of hand motor imagery on spinal excitability. This difference may be attributable to differences in how the H-reflex and F-wave are elicited. The H-reflex is evoked by electrical stimulation of group Ia afferents and is thought to be mainly monosynaptic in origin. The H-reflex size can be altered by spinal motoneuron excitability as well as mechanisms acting on the afferent volley (Pierrot-Deseilligny and Burke, 2005). On the other hand, the F-wave is caused by antidromic activation of the spinal motoneurons (Mercuri *et al*., 1996) and solely depends on the excitability of spinal motoneurons, though the sensitivity of the F-wave to changes in the spinal motoneuronal excitability is much less than the H-reflex (Espiritu *et al*., 2003). While the effect of hand motor imagery on spinal excitability is still under debate, the present results indicate that hand motor imagery involving ERD has a potent effect on the excitability of a limited portion of spinal motoneurons.

3.4.4 Physiological Interpretation of Event-Related Desynchronization during Motor Imagery

The neural network that generates rhythmic EEG activity consists of four elements: ITR neurons, TCR neurons, corticothalamic neurons, and inhibitory local circuit neurons in thalamus (Klimesch *et al*., 2007). In particular, ITR neurons, which express $GABA_A$ receptors (Widen *et al*., 1992), play a key role in the control of rhythmic EEG activity in

the mammalian brain (Steriade and Llinás, 1988). The alpha and beta bands EEG occur over the sensorimotor areas, indicating motor quiescence and a functionally inhibitory mode of the thalamocortical loops (Sterman and Clemente, 1962). Motor imagery or motor action decreases the alpha and beta bands EEG recorded over the sensorimotor areas (termed ERD). ERD is considered to reflect a decrease in synchrony of the underlying neuronal populations (Pfurtscheller, 1992).

Based on these findings, Pfurtscheller and Lopes da Silva (1999) created a model of ERD involving a relationship between ITR neurons, TCR neurons and cholinergic excitatory modulatory input from the brain stem. Using a computational model of thalamo-cortical networks, Suffczynski *et al*. (1999) reported that increased modulating input from the brain stem induced ERD, with an increase of TCR cells excitability and a decrease of ITR cells excitability (i.e., $GABA_A$ transmission was inhibited). In addition to these studies, the results presented in this dissertation suggested that hand motor imagery accompanied by ERD lead to a down-regulation of $GABA_A$ transmission in the human M1, and the ERD magnitude reflects the excitabilities of both the M1 and spinal motoneurons.

Changes in neural activity related to the generation of ERD during hand motor imagery are depicted schematically in Figure 3-7. The TCR neurons send excitatory inputs to the ITR neurons and M1, and receive cholinergic excitatory modulatory inputs from the brain stem. The ITR neurons project GABAergic inhibitory fibers to the TCR neurons. Therefore, the negative feedback loop formed by the TCR neurons and ITR neurons is involved in controlling the basic rhythmic activities of EEG during a rest condition. When a participant begins to perform a motor imagery or anticipate movement, the excitatory modulatory inputs from the brain stem and ascending afferent are increased. Increased excitatory input enhances TCR cell excitability, and this augmentation of the excitatory

inputs to the M1 induces a change in the ongoing EEG in the form of an ERD. As TMS stimulates the cortical pyramidal neurons indirectly via the cortical interneurons, which produce the indirect corticospinal waves (I-waves) (Lemon, 2002), the present results suggests that ERD during motor imagery induces a significant disinhibition of the I-wave generating neurons and a significant increase in the excitability of pyramidal neurons in the M1. Since the M1 neurons make monosynaptic connections on spinal motoneurons, an increase of the M1 excitability induced by motor imagery tasks involving ERD might enhance the subthreshold activation of spinal motoneurons. Moreover, ERD at Cz, C3, and P3 channels were significantly larger in the apparent F-wave trials compared with the non F-wave trials. This result suggested that not only the increase in the M1 excitability but also the activation of the non-primary motor areas were crucial for increasing spinal motoneuron excitability by hand motor imagery, though the physiological meaning of ERD at the non-primary motor areas are still under debate.

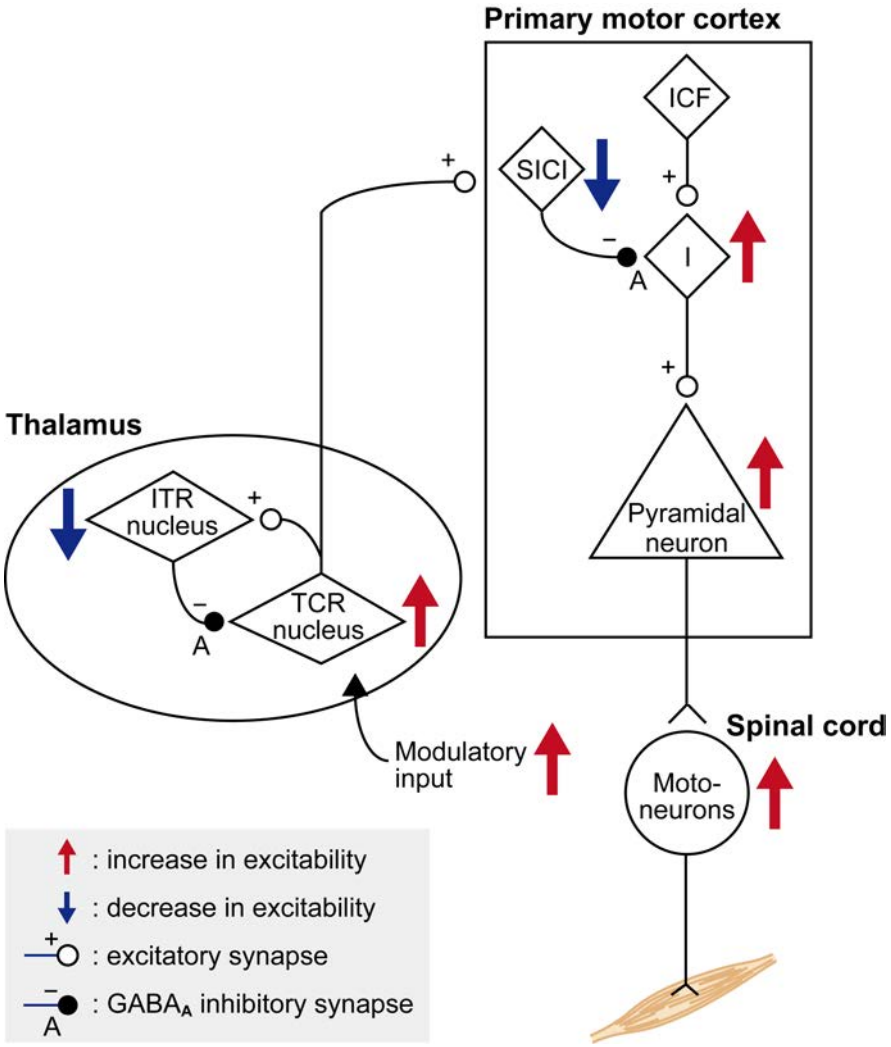

Figure 3-7. Schematic diagram of the neural activity changes related to the generation of ERD during motor imagery

Motor imagery accompanied by ERD over the sensorimotor area induced a significant inhibition of $GABA_A$ transmission in both the thalamus and M1, and a significant facilitation of the excitatory modulatory input, the TCR nucleus, and the I-wave generating neurons (I), resulting in an increase in the excitability of the M1 pyramidal neurons and spinal motoneurons.

Chapter 4

Conclusions

The purpose of the research presented in this dissertation was to investigate whether ERD in scalp EEG is a proper biomarker representing the excitability of the corticospinal system. Previous studies generally utilized two types of experimental techniques for the examination of the physiological characteristics of ERD. One is the simultaneous EEG-fMRI, which is able to compare the suppression of EEG oscillation with hemodynamic cortical activity. The other is the random timing TMS applied in conjunction with EEG recording, and examines the correlation between the TMS measurements (e.g., MEP amplitude) and feature values calculated from EEG signals (e.g., ERD). However, the hemodynamic activity may not monotonically reflect the electric cortical excitability. Random timing TMS with EEG recording requires large number of stimuli for assessing the correlation. In the present study, TMS was triggered by the instantaneous ERD magnitude calculated from the ongoing EEG. This method succeeded in finding a direct relationship between ERD and TMS measurements by using one-third less stimuli than the methods in the previous studies. Since EEG oscillation in specific frequency bands is believed to reflect a temporal framework for learning (Miltner *et al*., 1999), cognition (Thut and Miniussi, 2009), and motor control (Hummel *et al*., 2002), EEG-guided neurostimulation would be a powerful tool to investigate the frequency-dependent effects of oscillations on information processing in the brain.

In the first study (presented in Chapter 2), the association of sensorimotor EEG changes reflected by an ERD with the M1 excitability during kinesthetic motor imagery of the agonist

muscle contraction was examined using single and paired pulse TMS. Results showed that the ERD magnitude during motor imagery was associated with an increase of MEP amplitude and a decrease of SICI in the M1. Although the corticospinal circuits controlling wrist flexors would not be equivalent to those controlling wrist extensors, these tendencies were similar to the results obtained from FCR and ECR muscles. Furthermore, a decrease of SICI was prominently correlated with the ERD magnitude in the frequency range displaying the largest ERD in the screening session than that of the alpha and beta bands. Overall, I concluded that ERD magnitude in the frequency band displaying the largest ERD in the initial motor imagery condition reflects the M1 excitability of agonist muscle during motor imagery regardless of whether they are flexor or extensor.

The second study (presented in Chapter 3) tested the relationship between ERD magnitude during kinesthetic motor imagery of agonist muscle contraction and the excitability of spinal motoneurons, since increased M1 excitability associated with an ERD during motor imagery may induce a leaked cortical volley. It is further possible to facilitate spinal motoneurons without overt muscle contractions. I used F-wave as a measure of the excitability of spinal motoneurons, and compared F-wave measurements among three different ERD magnitudes. The main finding was that ERD during motor imagery was associated with an increase of F-wave persistence. It leads to suggest that ERD is a biomarker representing the increase in the excitability of both the M1 and spinal motoneurons. Comparison of the difference in the ERD topography between the apparent F-wave trials and non F-wave trials illustrated that ERD over both the primary sensorimotor and higher motor cortices were significantly larger in the apparent F-wave condition. This result suggested a contribution of the activity in the higher motor cortices in increasing spinal excitability by motor imagery, though the functional significance of ERD over the

non-primary motor areas are still under debate. Future study, in which spinal motoneuronal excitability is tested during motor imagery with suppressed activity of the higher motor cortices, would contribute to the understanding of the physiological basis of motor imagery and its influence on the corticospinal system.

In summary, the research presented in this dissertation revealed that ERD magnitude during kinesthetic motor imagery of agonist muscle contraction represents the excitabilities of both the contralateral M1 and ipsilateral spinal motoneurons. The present results indicated that motor imagery involving ERD increases the M1 excitability by decreasing the activity of GABAergic inhibitory interneurons, and thus, possesses the potential to induce subliminal central drives, which evoke descending volleys in the corticomotoneurons below the threshold for overt muscle movement. I, therefore, speculated that motor imagery task involving ERD induces changes in the corticospinal excitability similar to changes accompanying actual movements.

The present findings also suggest that the BCI system that provides immediate sensory feedback contingent upon the contralateral sensorimotor ERD involves the simultaneous activation of inputs and outputs to both the motor cortices and spinal motoneurons, triggering Hebbian-like plasticity in these regions. By repeated use of the BCI, users may learn to control brain oscillatory activity related to the cortical and spinal excitabilities, which is translated into a reaching and grasping movement of the paretic limb, in the framework of reinforcement learning. In this context, although the ERD-based BCI system has attracted attention as a new intervention for stroke rehabilitation, the results presented in this dissertation open up new possibilities for the use of the BCI system in the area of rehabilitation engineering. BCI would become a novel tool for rehabilitation in patients with severe spinal cord injury. Furthermore, since I provided evidence that the motor-related EEG

components reflect the actual neural activity, it encourages further development of BCI as a neurorehabilitation system for various types of neural deficits.

Acknowledgement

I would like to thank all the people who have helped and inspired me during my Ph.D. experiments and the writing of this dissertation. I particularly appreciate:

My supervisors:
Associate Professor **Junichi Ushiba** for leading me into the world of science and for his continuous support, inspiration, and friendship as well as for his creativity and enthusiasm. I would like to show my deepest gratitude to him.
Senior Team Leader **Atsushi Iriki** for introducing me to research using non-human primates, helping me to become a more independent scientist, and for sharing his vast knowledge and experience.

My committee members:
Professor Emeritus **Yutaka Tomita**, Professor **Kotaro Oka**, and Associate Professor **Akira Funahashi** for their valuable comments on my Ph.D. thesis and their lectures on bioscience and informatics from the time I was a bachelor student.

My advisors:
Associate Professor **Junichi Ushiyama** for many long discussions and thoughtful suggestions on my Ph.D. experiments.
Research Associate **Shoko Kasuga** for generously sharing her knowledge about motor control and motor learning research.
Professor **Yoshihisa Masakado** and Professor **Meigen Liu** for their technical advice on my Ph.D. experiments and insightful comments, which have helped me to improve the quality of my original manuscripts significantly.

All the current and past members of Ushiba laboratory, particularly the following:
Dr. **Takashi Ono** and Dr. **Chadwick Boulay** for giving helpful advice on EEG analysis and helping in EEG measurements and construction of the experimental system.
Chie Habagishi, **Ryosuke Matsuya**, **Toma Onose**, **Misa Oto**, and **Yoshihiro Watanabe**, who were my lab-mates from April 2010 to March 2013. I am deeply grateful for their warm encouragement whenever I confronted difficulties.
Tomofumi Sekiguchi, **Akito Kosugi**, **Kenta Sato**, and **Takafumi Nakamura** for their help with the primate research and for being fun.
Sayoko Ishii for taking care of a variety of paperwork and administrative procedures. It enabled me to conduct my Ph.D. experiments without any obstacles.

All members of Iriki laboratory, particularly the following:
Dr. **Miki Taoka** for many valuable suggestions about developing the cortical stimulator and for teaching me the techniques for acute animal experiments.
Dr. **Yumiko Yamazaki**, **Masakado Saiki**, **Masayuki Inada**, and **Taku Koike** for helping to keep the postoperative marmosets in good health.

My collaborators in Japan:
Dr. **Kimika Yoshino** and **Takahiro Kondo** for their assistance with the animal surgery and advice on primate postoperative care.
Professor **Hideyuki Okano** and Professor **Hirotaka J Okano** for their academic suggestions and firm support for my primate research.

My collaborators in Italy:
Dr. **Banty Tia** for assistance on the task training of marmosets and postoperative care. We shared the same marmosets for each experiment, and our 10-month collaboration in Japan was an outstanding experience for me.
Dr. **Elisa Castagnola** and Dr. **Alberto Ansaldo** for developing cortical electrodes that are perfectly compatible with the marmoset brain.
Professor **Luciano Fadiga** and Dr. **Davide Ricci** for supporting my stay at the Italian Institute of Technology and for lending the multichannel stimulator.

I would like to express my gratitude to Professor **Kazuo Tanishita**. Your lecture on biomedical engineering that I listened to when I was a junior high school student inspired me to become a scientist. If I had not met you, I would not have been a Ph.D degree holder.

I want to thank all my non-scientist friends, and special thanks go to **Miyuki Sugisaki** whose love and support always motivated me. Thank you for being there for me.

Special thanks also go to my family, **Yuri** and **Sakiko Takemi** and **Minoru** and **Itsuko Sasayama**, who supported me every day and encouraged me to strive toward my goal.

Lastly, and most importantly, I wish to thank my parents, **Hiromitsu** and **Yukari Takemi**, for their unflagging love and continuous support throughout my life. Without them many things would have been impossible and they have made me who I am today.

To them I dedicate this dissertation.

References

Abbruzzese G, Trompetto C, Schieppati M. The excitability of the human motor cortex increases during execution and mental imagination of sequential but not repetitive finger movements. *Exp Brain Res*. 1996;111:465–472.

Alegre M, Labarga A, Gurtubay IG, Iriarte J, Malanda A, Artieda J. Movement-related changes in cortical oscillatory activity in ballistic, sustained and negative movements. *Exp Brain Res*. 2003;148:17–25.

Ang KK, Chua KSG, Phua KS, Wang C, Chin ZY, Kuah CWK, Low W, Guan C. A Randomized Controlled Trial of EEG-Based Motor Imagery Brain-Computer Interface Robotic Rehabilitation for Stroke. *Clin EEG Neurosci*. 2014; [published online ahead of print].

Ang KK, Guan C, Chua KSG, Ang BT, Kuah CWK, Wang C, Phua KS, Chin ZY, Zhang H. A large clinical study on the ability of stroke patients to use an EEG-based motor imagery brain-computer interface. *Clin EEG Neurosci*. 2011;42:253–258.

Babiloni C, Carducci F, Cincotti F, Rossini PM, Neuper C, Pfurtscheller G, Babiloni F. Human movement-related potentials vs desynchronization of EEG alpha rhythm: a high-resolution EEG study. *Neuroimage*. 1999;10:658–665.

Buch ER, Weber C, Cohen LG, Braun C, Dimyan MA, Ard T, Mellinger J, Caria A, Soekadar S, Fourkas A, Birbaumer N. Think to move: a neuromagnetic brain-computer interface (BCI) system for chronic stroke. *Stroke*. 2008;39:910–917.

Buzsáki G, Anastassiou CA, Koch C. The origin of extracellular fields and currents - EEG, ECoG, LFP and spikes. *Nat Rev Neurosci*. 2012;13:407–420.

Chen R. Interactions between inhibitory and excitatory circuits in the human motor cortex. *Exp Brain Res*. 2004;154:1–10.

Chen R, Tam A, Bütefisch C, Corwell B, Ziemann U, Rothwell JC, Cohen LG. Intracortical inhibition and facilitation in different representations of the human motor cortex. *J Neurophysiol*. 1998;80:2870–2881.

Chen X, Scangos KW, Stuphorn V. Supplementary motor area exerts proactive and reactive control of arm movements. *J Neurosci*. 2010;30:14657–14675.

Cheney PD, Fetz EE, Palmer SS. Patterns of facilitation and suppression of antagonist forelimb muscles from motor cortex sites in the awake monkey. *J Neurophysiol*. 1985;53:805–820.

Chye L, Nosaka K, Murray L, Edwards D, Thickbroom G. Corticomotor excitability of wrist flexor and extensor muscles during active and passive movement. *Hum Mov Sci*. 2010;29:494–501.

Cohen LG, Roth BJ, Wassermann EM, Topka H, Fuhr P, Schultz J, Hallett M. Magnetic stimulation of the human cerebral cortex, an indicator of reorganization in motor pathways in certain pathological conditions. *J Clin Neurophysiol*. 1991;8:56–65.

Daly JJ, Wolpaw JR. Brain-computer interfaces in neurological rehabilitation. *Lancet Neurol*. 2008;7:1032–1043.

Day BL, Dressler D, Maertens de Noordhout A, Marsden CD, Nakashima K, Rothwell JC, Thompson PD. Electric and magnetic stimulation of human motor cortex: surface EMG and single motor unit responses. *J Physiol (Lond)*. 1989;412:449–473.

Decety J. The neurophysiological basis of motor imagery. *Behav Brain Res*. 1996;77:45–52.

Dechent P, Merboldt K-D, Frahm J. Is the human primary motor cortex involved in motor imagery? *Cogn Brain Res*. 2004;19:138–144.

Dum RP, Strick PL. The origin of corticospinal projections from the premotor areas in the frontal lobe. *J Neurosci*. 1991;11:667–689.

Espiritu MG, Lin CS-Y, Burke D. Motoneuron excitability and the F wave. *Muscle Nerve*. 2003;27:720–727.

Facchini S, Muellbacher W, Battaglia F, Boroojerdi B, Hallett M. Focal enhancement of motor cortex excitability during motor imagery: a transcranial magnetic stimulation study. *Acta Neurol Scand*. 2002;105:146–151.

Fetz EE, Cheney PD. Postspike facilitation of forelimb muscle activity by primate corticomotoneuronal cells. *J Neurophysiol*. 1980;44:751–772.

Fierro B, Raimondo D, Modica A. F-wave study at different stimulation rates. *Electromyogr Clin Neurophysiol*. 1991;31:357–360.

Formaggio E, Storti SF, Cerini R, Fiaschi A, Manganotti P. Brain oscillatory activity during motor imagery in EEG-fMRI coregistration. *Magn Reson Imaging*. 2010;28:1403–1412.

Formaggio E, Storti SF, Avesani M, Cerini R, Milanese F, Gasparini A, Acler M, Mucelli RP, Fiaschi A, Manganotti P. EEG and FMRI coregistration to investigate the cortical oscillatory activities during finger movement. *Brain Topogr*. 2008;21:100–111.

Fujisawa R, Kimura J, Taniguchi S, Ichikawa H, Hara M, Shimizu H, Iida H, Yamada T, Tani T. Effect of volitional relaxation and motor imagery on F wave and MEP: do these tasks affect excitability of the spinal or cortical motor neurons? *Clin Neurophysiol*. 2011;122:1405–1410.

Gandevia SC, Wilson LR, Inglis JT, Burke D. Mental rehearsal of motor tasks recruits alpha-motoneurones but fails to recruit human fusimotor neurones selectively. *J Physiol (Lond)*. 1997;505:259–266.

Gao Q, Duan X, Chen H. Evaluation of effective connectivity of motor areas during motor imagery and execution using conditional Granger causality. *Neuroimage*. 2011;54:1280–1288.

Gerloff C, Bushara K, Sailer A, Wassermann EM, Chen R, Matsuoka T, Waldvogel D, Wittenberg GF, Ishii K, Cohen LG, Hallet M. Multimodal imaging of brain reorganization in motor areas of the contralesional hemisphere of well recovered patients after capsular stroke. *Brain*. 2006;129:791–808.

Gold JI, Shadlen MN. The neural basis of decision making. *Annu Rev Neurosci*. 2007;30:535–574.

Goldring S, Ratcheson R. Human motor cortex: sensory input data from single neuron recordings. *Science*. 1972;175:1493–1495.

Haggard P. Human volition: towards a neuroscience of will. *Nat Rev Neurosci*. 2008;9:934–946.

Halder S, Agorastos D, Veit R, Hammer EM, Lee S, Varkuti B, Bogdan M, Rosenstiel W, Birbaumer N, Kübler A. Neural mechanisms of brain-computer interface control. *Neuroimage*. 2011;55:1779–1790.

Hara M, Kimura J, Walker DD, Taniguchi S, Ichikawa H, Fujisawa R, Shimizu H, Abe T, Yamada T, Kayamori R, Mizutani T. Effect of motor imagery and voluntary muscle contraction on the F wave. *Muscle Nerve*. 2010;42:208–212.

Hashimoto R, Rothwell JC. Dynamic changes in corticospinal excitability during motor imagery. *Exp Brain Res*. 1999;125:75–81.

Herwig U, Satrapi P, Schönfeldt-Lecuona C. Using the international 10-20 EEG system for positioning of transcranial magnetic stimulation. *Brain Topogr*. 2003;16:95–99.

Hjorth B. An on-line transformation of EEG scalp potentials into orthogonal source derivations. *Electroencephalogr Clin Neurophysiol*. 1975;39:526–530.

Hultborn H, Nielsen JB. H-reflexes and F-responses are not equally sensitive to changes in motoneuronal excitability. *Muscle Nerve*. 1995;18:1471–1474.

Hummel FC, Andres F, Altenmüller E, Dichgans J, Gerloff C. Inhibitory control of acquired motor programmes in the human brain. *Brain*. 2002;125:404–420.

Ichikawa H, Kimura J, Taniguchi S, Hara M, Fujisawa R, Shimizu H, Yamada T, Kawamura M. Motor imagery facilitates the spinal motor neurons without hemispheric asymmetry. *J Clin Neurophysiol*. 2009;26:358–365.

Izumi S, Koyama Y, Furukawa T, Ishida A. Effect of antagonistic voluntary contraction on motor responses in the forearm. *Clin Neurophysiol*. 2000;111:1008–1014.

Jackson PL, Lafleur MF, Malouin F, Richards C, Doyon J. Potential role of mental practice using motor imagery in neurologic rehabilitation. *Arch Phys Med Rehabil*. 2001;82:1133–1141.

Jasper HH. The ten-twenty electrode system of the International Federation. *Electroencephalogr Clin Neurophysiol*. 1958;10:371–375.

Kalaska JF, Rizzolatti G. Voluntary movement: the primary motor cortex. In: *Principles of Neural Science 5th ed*., edited by Kandel ER, Schwartz JH, Jessell TM, Siegelbaum SA, Hudspeth AJ. New York: McGraw-Hill, 2013, p.835–864.

Kasai T, Kawai S, Kawanishi M, Yahagi S. Evidence for facilitation of motor evoked potentials (MEPs) induced by motor imagery. *Brain Res*. 1997;744:147–150.

Kasser RJ, Cheney PD. Characteristics of corticomotoneuronal postspike facilitation and reciprocal suppression of EMG activity in the monkey. *J Neurophysiol*. 1985;53:959–978.

Kiers L, Fernando B, Tomkins D. Facilitatory effect of thinking about movement on magnetic motor-evoked potentials. *Electroencephalogr Clin Neurophysiol*. 1997;105:262–268.

Klimesch W, Sauseng P, Hanslmayr S. EEG alpha oscillations: the inhibition-timing hypothesis. *Brain Res Rev*. 2007;53:63–88.

Kobayashi M, Pascual-Leone A. Transcranial magnetic stimulation in neurology. *Lancet Neurol*. 2003;2:145–156.

Kujirai T, Caramia MD, Rothwell JC, Day BL, Thompson PD, Ferbert A, Wroe S, Asselman P, Marsden CD. Corticocortical inhibition in human motor cortex. *J Physiol (Lond)*. 1993;471:501–519.

Di Lazzaro V, Profice P, Ranieri F, Capone F, Dileone M, Oliviero A, Pilato F. I-wave origin and modulation. *Brain Stimul*. 2012;5:512–525.

Lemon R. Basic physiology of transcranial magnetic stimulation. In: *Handbook of Transcranial Magnetic Stimulation,* edited by Pascual-Leone A, Davey NJ, Rothwell J, Wassermann EM, Puri BK. London: Arnold, 2002, p. 61–77.

Lemon RN, Kirkwood PA, Maier MA, Nakajima K, Nathan P. Direct and indirect pathways for corticospinal control of upper limb motoneurons in the primate. *Prog Brain Res*. 2004;143:263–279.

Levin O, Steyvers M, Wenderoth N, Li Y, Swinnen SP. Dynamical changes in corticospinal excitability during imagery of unimanual and bimanual wrist movements in humans: a transcranial magnetic stimulation study. *Neurosci Lett*. 2004;359:185–189.

Lin JZ, Floeter MK. Do F-wave measurements detect changes in motor neuron excitability? *Muscle Nerve*. 2004;30:289–294.

Lotze M, Halsband U. Motor imagery. *J Physiol (Paris)*. 2006;99:386–395.

Mäki H, Ilmoniemi RJ. EEG oscillations and magnetically evoked motor potentials reflect motor system excitability in overlapping neuronal populations. *Clin Neurophysiol*. 2010;121:492–501.

McMillan S, Nougier V, Byblow WD. Human corticospinal excitability during a precued reaction time paradigm. *Exp Brain Res*. 2004;156:80–87.

McNeil CJ, Butler JE, Taylor JL, Gandevia SC. Testing the excitability of human motoneurons. *Front Hum Neurosci*. 2013;7:152.

Mercuri B, Wassermann EM, Manganotti P, Ikoma K, Samii A, Hallett M. Cortical modulation of spinal excitability: an F-wave study. *Electroencephalogr Clin Neurophysiol*. 1996;101:16–24.

Miltner WH, Braun C, Arnold M, Witte H, Taub E. Coherence of gamma-band EEG activity as a basis for associative learning. *Nature*. 1999;397:434–436.

Mukaino M, Ono T, Shindo K, Fujiwara T, Ota T, Kimura A, Liu M, Ushiba J. Efficacy of brain-computer interface-driven neuromuscular electrical stimulation for chronic paresis after stroke. *J Rehabil Med*. 2014;46:378–382.

Naito E, Kochiyama T, Kitada R, Nakamura S, Matsumura M, Yonekura Y, Sadato N. Internally simulated movement sensations during motor imagery activate cortical motor areas and the cerebellum. *J Neurosci*. 2002;22:3683–3691.

Neubert F-X, Mars RB, Buch ER, Olivier E, Rushworth MFS. Cortical and subcortical interactions during action reprogramming and their related white matter pathways. *Proc Natl Acad Sci USA*. 2010;107:13240–13245.

Neuper C, Scherer R, Reiner M, Pfurtscheller G. Imagery of motor actions: differential effects of kinesthetic and visual-motor mode of imagery in single-trial EEG. *Cogn Brain Res*. 2005;25:668–677.

Neuper C, Pfurtscheller G. Motor imagery and ERD. In: *Event-Related Desynchronization. Handbook of Electroencephalography and Clinical Neurophysiology*, edited by Pfurtscheller G, Lopes da Silva FH. Amsterdam: Elsevier, 1999, vol. 6, p. 303–326.

Nikolova M, Pondev N, Christova L, Wolf W, Kossev AR. Motor cortex excitability changes preceding voluntary muscle activity in simple reaction time task. *Eur J Appl Physiol*. 2006;98:212–219.

Ono T, Shindo K, Kawashima K, Ota N, Ito M, Ota T, Mukaino M, Fujiwara T, Kimura A, Liu M, Ushiba J. Brain-computer interface with somatosensory feedback improves functional recovery from severe hemiplegia due to chronic stroke. *Front Neuroeng*. 2014;7:19.

Ono T, Kimura A, Ushiba J. Daily training with realistic visual feedback improves reproducibility of event-related desynchronisation following hand motor imagery. *Clin Neurophysiol*. 2013;124:1779–1786.

Pascual-Leone A, Valls-Solé J, Wassermann EM, Hallett M. Responses to rapid-rate transcranial magnetic stimulation of the human motor cortex. *Brain*. 1994;117:847–858.

Patuzzo S, Fiaschi A, Manganotti P. Modulation of motor cortex excitability in the left hemisphere during action observation: a single- and paired-pulse transcranial magnetic stimulation study of self- and non-self-action observation. *Neuropsychologia*. 2003;41:1272–1278.

Pfurtscheller G, Daly I, Bauernfeind G, Müller-Putz GR. Coupling between intrinsic prefrontal HbO2 and central EEG beta power oscillations in the resting brain. *PLoS ONE*. 2012;7:e43640.

Pfurtscheller G, Brunner C, Schlögl A, Lopes da Silva FH. Mu rhythm (de)synchronization and EEG single-trial classification of different motor imagery tasks. *Neuroimage*. 2006;31:153–159.

Pfurtscheller G. The cortical activation model (CAM). *Prog Brain Res*. 2006;159:19–27.

Pfurtscheller G, Graimann B, Huggins JE, Levine SP, Schuh LA. Spatiotemporal patterns of beta desynchronization and gamma synchronization in corticographic data during self-paced movement. *Clin Neurophysiol*. 2003;114:1226–1236.

Pfurtscheller G, Lopes da Silva FH. Event-related EEG/MEG synchronization and desynchronization: basic principles. *Clin Neurophysiol*. 1999;110:1842–1857.

Pfurtscheller G, Stancák A, Neuper C. Event-related synchronization (ERS) in the alpha band--an electrophysiological correlate of cortical idling: a review. *Int J Psychophysiol*. 1996;24:39–46.

Pfurtscheller G. Event-related synchronization (ERS): an electrophysiological correlate of cortical areas at rest. *Electroencephalogr Clin Neurophysiol*. 1992;83:62–69.

Pierrot-Deseilligny E, Burke D. *The Circuitry of the Human Spinal Cord. Its Role in Motor Control and Movement Disorders*. Cambridge: Cambridge Univ. Press, 2005.

Poldrack RA, Mumford JA, Nichols TE. *Handbook of Functional MRI Data Analysis*. Cambridge: Cambridge Univ. Press, 2011.

Porro CA, Francescato MP, Cettolo V, Diamond ME, Baraldi P, Zuiani C, Bazzocchi M, di Prampero PE. Primary motor and sensory cortex activation during motor performance and motor imagery: a functional magnetic resonance imaging study. *J Neurosci*. 1996;16:7688–7698.

Quartarone A, Bagnato S, Rizzo V, Morgante F, Sant'Angelo A, Battaglia F, Messina C, Siebner HR, Girlanda P. Distinct changes in cortical and spinal excitability following high-frequency repetitive TMS to the human motor cortex. *Exp Brain Res*. 2005;161:114–124.

Ramos-Murguialday A, Broetz D, Rea M, Läer L, Yilmaz O, Brasil FL, Liberati G, Curado MR, Garcia-Cossio E, Vyziotis A, Cho W, Agostini M, Soares E, Soekadar S, Caria A, Cohen LG, Birbaumer N. Brain-machine interface in chronic stroke rehabilitation: a controlled study. *Ann Neurol*. 2013;74:100–108.

Reynolds C, Ashby P. Inhibition in the human motor cortex is reduced just before a voluntary contraction. *Neurology*. 1999;53:730–735.

Riccio I, Iolascon G, Barillari MR, Gimigliano R, Gimigliano F. Mental practice is effective in upper limb recovery after stroke: a randomized single-blind cross-over study. *Eur J Phys Rehabil Med*. 2010;46:19–25.

Ridding MC, Rothwell JC. Is there a future for therapeutic use of transcranial magnetic stimulation? *Nat Rev Neurosci*. 2007;8:559–567.

Ritter P, Moosmann M, Villringer A. Rolandic alpha and beta EEG rhythms' strengths are inversely related to fMRI-BOLD signal in primary somatosensory and motor cortex. *Hum Brain Mapp*. 2009;30:1168–1187.

Rivner MH. The use of F-waves as a probe for motor cortex excitability. *Clin Neurophysiol*. 2008;119:1215–1216.

Rizzolatti G, Strick PL. The neural basis of cognition. In: *Principles of Neural Science 5th ed*., edited by Kandel ER, Schwartz JH, Jessell TM, Siegelbaum SA, Hudspeth AJ. New York: McGraw-Hill, 2013, p.412–425.

Rossi S, Pasqualetti P, Tecchio F, Pauri F, Rossini PM. Corticospinal excitability modulation during mental simulation of wrist movements in human subjects. *Neurosci Lett*. 1998;243:147–151.

Rossini PM, Rossi S, Pasqualetti P, Tecchio F. Corticospinal excitability modulation to hand muscles during movement imagery. *Cereb Cortex*. 1999;9:161–167.

Rossini PM, Barker AT, Berardelli A, Caramia MD, Caruso G, Cracco RQ, Dimitrijević MR, Hallett M, Katayama Y, Lücking CH, Maertens de Noordhout AL, Marsden CD, Murray NMF, Rothwell JC, Swash M, Tomberg C. Non-invasive electrical and magnetic stimulation of the brain, spinal cord and roots: basic principles and procedures for routine clinical application. Report of an IFCN committee. *Electroencephalogr Clin Neurophysiol*. 1994;91:79–92.

Sanger TD, Garg RR, Chen R. Interactions between two different inhibitory systems in the human motor cortex. *J Physiol (Lond)*. 2001;530:307–317.

Sauseng P, Klimesch W, Gerloff C, Hummel FC. Spontaneous locally restricted EEG alpha activity determines cortical excitability in the motor cortex. *Neuropsychologia*. 2009;47:284–288.

Schulz H, Ubelacker T, Keil J, Müller N, Weisz N. Now I am Ready--Now I am not: The Influence of Pre-TMS Oscillations and Corticomuscular Coherence on Motor-Evoked Potentials. *Cereb Cortex*. 2013;24:1708–1719.

Shadlen MN, Newsome WT. Neural basis of a perceptual decision in the parietal cortex (area LIP) of the rhesus monkey. *J Neurophysiol*. 2001;86:1916–1936.

Shindo K, Kawashima K, Ushiba J, Ota N, Ito M, Ota T, Kimura A, Liu M. Effects of neurofeedback training with an electroencephalogram-based Brain-Computer Interface for hand paralysis in patients with chronic stroke: A preliminary case series study. *J Rehabil Med*. 2011;43:951–957.

Soekadar SR, Birbaumer N, Slutzky MW, Cohen LG. Brain-machine interfaces in neurorehabilitation of stroke. *Neurobiol Dis*. 2014; [published online ahead of print].

Sohn YH, Dang N, Hallett M. Suppression of corticospinal excitability during negative motor imagery. *J Neurophysiol*. 2003;90:2303–2309.

Steriade M, Llinás RR. The functional states of the thalamus and the associated neuronal interplay. *Physiol Rev*. 1988;68:649–742.

Sterman MB, Clemente CD. Forebrain inhibitory mechanisms: cortical synchronization induced by basal forebrain stimulation. *Exp Neurol*. 1962;6:91–102.

Stinear CM, Byblow WD, Steyvers M, Levin O, Swinnen SP. Kinesthetic, but not visual, motor imagery modulates corticomotor excitability. *Exp Brain Res*. 2006;168:157–164.

Suffczynski P, Pijn JP, Pfurtscheller G, Lopes da Silva FH. Event-related dynamics of alpha band rhythms: a neuronal network model of focal ERD/surround ERD. In: *Event-Related Desynchronization. Handbook of Electroencephalography and Clinical Neurophysiology*, edited by Pfurtscheller G, Lopes da Silva FH. Amsterdam: Elsevier, 1999, vol. 6, p. 67–85.

Taniguchi S, Kimura J, Yamada T, Ichikawa H, Hara M, Fujisawa R, Shimizu H, Tani T. Effect of motion imagery to counter rest-induced suppression of F-wave as a measure of anterior horn cell excitability. *Clin Neurophysiol*. 2008;119:1346–1352.

Teitti S, Määttä S, Säisänen L, Könönen M, Vanninen R, Hannula H, Mervaala E, Karhu J. Non-primary motor areas in the human frontal lobe are connected directly to hand muscles. *Neuroimage*. 2008;40:1243–1250.

Thut G, Miniussi C. New insights into rhythmic brain activity from TMS-EEG studies. *Trends Cogn Sci*. 2009;13:182–189.

Vargas CD, Olivier E, Craighero L, Fadiga L, Duhamel JR, Sirigu A. The influence of hand posture on corticospinal excitability during motor imagery: a transcranial magnetic stimulation study. *Cereb Cortex*. 2004;14:1200–1206.

Varkuti B, Guan C, Pan Y, Phua KS, Ang KK, Kuah CW, Chua K, Ang BT, Birbaumer N, Sitaram R. Resting State Changes in Functional Connectivity Correlate With Movement Recovery for BCI and Robot-Assisted Upper-Extremity Training After Stroke. *Neurorehabil Neural Repair*. 2012;27:53–62.

Wisden W, Laurie DJ, Monyer H, Seeburg PH. The distribution of 13 GABAA receptor subunit mRNAs in the rat brain. I. Telencephalon, diencephalon, mesencephalon. *J Neurosci*. 1992;12:1040–1062.

Yahagi S, Kasai T. Facilitation of motor evoked potentials (MEPs) in first dorsal interosseous (FDI) muscle is dependent on different motor images. *Electroencephalogr Clin Neurophysiol*. 1998;109:409–417.

Young BM, Nigogosyan Z, Walton LM, Song J, Nair VA, Grogan SW, Tyler ME, Edwards DF, Caldera K, Sattin JA, Williams JC, Prabhakaran V. Changes in functional brain organization and behavioral correlations after rehabilitative therapy using a brain-computer interface. *Front Neuroeng*. 2014;7:26.

Yuan H, Liu T, Szarkowski R, Rios C, Ashe J, He B. Negative covariation between task-related responses in alpha/beta-band activity and BOLD in human sensorimotor cortex: an EEG and fMRI study of motor imagery and movements. *Neuroimage*. 2010;49:2596–2606.

Ziemann U, Chen R, Cohen LG, Hallett M. Dextromethorphan decreases the excitability of the human motor cortex. *Neurology*. 1998;51:1320–1324.

Ziemann U, Lönnecker S, Steinhoff BJ, Paulus W. Effects of antiepileptic drugs on motor cortex excitability in humans: a transcranial magnetic stimulation study. *Ann Neurol*. 1996;40:367–378.

Bibliography

1. Original Papers

[1] Mitsuaki Takemi, Yoshihisa Masakado, Meigen Liu, Junichi Ushiba. Sensorimotor event-related desynchronization represents the excitability of human spinal motoneurons. ***Neuroscience***, 297: 58-67, 2015.

[2] Mitsuaki Takemi, Takahiro Kondo, Kimika Yoshino-Saito, Tomofumi Sekiguchi, Akito Kosugi, Shoko Kasuga, Hirotaka J Okano, Hideyuki Okano, Junichi Ushiba. Three-dimensional motion analysis of arm-reaching movements in healthy and hemispinalized common marmosets. ***Behavioural Brain Research***, 275: 259-268, 2014.

[3] Mitsuaki Takemi, Yoshihisa Masakado, Meigen Liu, Junichi Ushiba. Event-related desynchronization reflects down-regulation of intracortical inhibition in human primary motor cortex. ***Journal of Neurophysiology***, 110(5): 1158-66, 2013.

2. International Conferences

[1] Mitsuaki Takemi, Elisa Castagnola, Alberto Ansaldo, Davide Ricci, Luciano Fadiga, Miki Taoka, Atsushi Iriki, Junichi Ushiba. A novel system for short-time sensorimotor mapping in animal experiments. ***The 44th Annual Meeting of the Society for Neuroscience***, Washington D.C., U.S.A. (November, 2014).

[2] Mitsuaki Takemi, Takahiro Kondo, Kimika Yoshino-Saito, Tomohumi Sekiguchi, Akito Kosugi, Hirotaka J Okano, Hideyuki Okano, Junichi Ushiba. Three dimensional motion analysis of food retrieval movement in common marmosets with cervical hemisection. ***The 43rd Annual Meeting of the Society for Neuroscience***, San Diego, U.S.A. (November, 2013).

[3] Takahiro Kondo, Kimika Yoshino-Saito, Mitsuaki Takemi, Tomohumi Sekiguchi, Akito Kosugi, Yamato Yoshihara, Yukio Nishimura, Tadashi Isa, Hirotaka J Okano, Masaya Nakamura, Junichi Ushiba, Hideyuki Okano. Corticospinal tract plasticity contributes to functional motor recovery after C4/5 lateral hemisection in common marmosets. ***The 43rd Annual Meeting of the Society for Neuroscience***, San Diego, U.S.A. (November, 2013).

[4] Mitsuaki Takemi, Yoshihisa Masakado, Meigen Liu, Junichi Ushiba. Is event-related desynchronization a biomarker representing corticospinal excitability? ***35th Annual International Conference of the IEEE Engineering in Medicine and Biology Society***, Osaka, Japan (July, 2013).

[5] Satoshi Inoue, Koichi Hara, Keigo Hikishima, Yuji Komaki, Toshio Itoh, Hiroshi Iwata, Mitsuaki Takemi, Junichi Ushiba, Hideo Tsukada, Hirotaka J Okano, Hideyuki Okano. Development of less invasive transient middle cerebral artery occlusion model on Common Marmoset for cell therapy. ***The 36th Annual Meeting of the Japan Neuroscience Society***, Kyoto, Japan (June, 2013).

[6] Mitsuaki Takemi, Yoshihisa Masakado, Meigen Liu, Junichi Ushiba. Association between cortico-cortical interaction and the magnitude of event-related desynchronization during hand motor imagery. ***The 36th Annual Meeting of the Japan Neuroscience Society***, Kyoto, Japan (June, 2013).

[7] Kimika Yoshino-Saito, Takahiro Kondo, Mitsuaki Takemi, Tomohumi Sekiguchi, Junichi Ushiba, Hirotaka J Okano, Hideyuki Okano. Behavioral tests in spontaneous motor recovery after C4/C5 spinal lesioned marmosets. ***The 36th Annual Meeting of the Japan Neuroscience Society***, Kyoto, Japan (June, 2013).

[8] Mitsuaki Takemi, Chadwick Bouley, Meigen Liu, Yoshihisa Masakado, Junichi Ushiba. A study on the physiological mechanism of event-related desynchronization by hand motor imagery – Evidence for BCI based neurorehabilitation. ***BMI Osaka 2012:The International Symposium on the Clinical Application of Brain-Machine Interfaces***, Osaka, Japan (October, 2012).

[9] Mitsuaki Takemi, Akio Kimura, Meigen Liu, Yoshihisa Masakado, Junichi Ushiba. Event-related desynchronization during hand motor imagery is correlated with excitability of both primary motor cortex and spinal motoneuron. ***The 42nd Annual Meeting of the Society for Neuroscience***, New Orleans, U.S.A. (October, 2012).

[10] Mitsuaki Takemi, Meigen Liu, Yoshihisa Masakado, Junichi Ushiba. Event-related desynchronization by hand motor imagery is associated with corticospinal excitability – A physiological evidence for brain-computer interface based neurorehabilitation. ***APRU-BMAP 2012***, Tokyo, Japan (August, 2012).

3. Domestic Conferences

[1] 吉野-斎藤紀美香、近藤崇弘、武見充晃、関口智史、小杉亮人、吉原也真人、西村幸男、伊佐正、岡野James洋尚、中村雅也、牛場潤一、岡野栄之. Corticospinal tract plasticity contributes to functional motor recovery after C4/5 lateral hemisection in common marmosets. ***第3回日本マーモセット研究会大会***、九州大学(福岡)、2013年12月.

[2] 近藤崇弘、吉野-斎藤紀美香、武見充晃、関口智史、牛場潤一、中村雅也、岡野James洋尚、岡野栄之. 脊髄損傷マーモセットの自然回復過程における運動機能解析. ***第2回日本マーモセット研究会大会***、慶應義塾大学三田キャンパス(東京)、2013年2月.

[3] 井上賢、原晃一、疋島啓吾、小牧裕司、伊藤豊志雄、岩田祐士、塚田秀夫、武見充晃、牛場潤一、岡野James洋尚、吉田一成、岡野栄之. マーモセットMCAOモデルにおける細胞治療を目標としたPET評価. ***日本脳神経外科学会第71回学術総会***、大阪国際会議場(大阪)、2012年10月.

[4] 武見充晃、里宇明元、正門由久、牛場潤一. 運動イメージ中に発生する事象関連脱同期量は皮質脊髄路の興奮性に相関する. ***第6回Motor Control研究会***、自然科学研究機構 岡崎コンファレンスセンター(愛知)、2012年6月.

[5] 武見充晃、木村彰男、里宇明元、正門由久、牛場潤一. 運動イメージ中に発生する事象関連脱同期は皮質内抑制の減弱を反映する指標となりうる. ***第41回日本臨床神経生理学会***、グランシップ(静岡)、2011年11月.

[6] 大藤美紗、武見充晃、鎌谷大樹、木村彰男、里宇明元、牛山潤一、牛場潤一. Brain-Machine Interfaceリハビリテーションへの視覚フィードバック、体性感覚フィードバックの導入. ***第41回日本臨床神経生理学会***、グランシップ(静岡)、2011年11月.

[7] 武見充晃、大藤美紗、鎌谷大樹、木村彰男、里宇明元、牛場潤一. Motor learning in closed-loop brain-machine interface increases excitability of sensorimotor cortex. ***第26回生体生理工学シンポジウム***、立命館大学びわこ・くさつキャンパス(滋賀)、2011年9月.

[8] 武見充晃、大藤美紗、鎌谷大樹、木村彰男、里宇明元、牛場潤一. 閉ループ型ブレイン・マシン・インターフェースが体性感覚運動野の興奮性におよぼす影響. ***MEとバイオサイバネティックス研究会***、北海道大学情報科学研究科(北海道)、2011年6月.

4. Awards

[1] The 10 top-ranked projects, ***the annual BCI research award 2012*** (August 2012). Project title: Online estimate of event-related desynchronization by hand motor imagery is associated with corticospinal excitability — Physiological evidence for brain-computer interface based neurorehabilitation.

5. Book Chapter

[1] Mitsuaki Takemi, Yoshihisa Masakado, Meigen Liu, Junichi Ushiba. Event-related desynchronization by hand motor imagery is associated with corticospinal excitability: physiological evidence for BCI based neurorehabilitation. In: *Christoph Guger, Brendan Z Allison, Eric C Leuthardt (Eds.), Brain-Computer Interface Research: A State-of-the-Art Summary-2*. Springer, Berlin, 2014, vol. 6, pp.85-94.

6. Review Article

[1] 武見充晃、牛場潤一. ブレイン・マシン・インターフェースによる脳の可塑的変化のメカニズム. ***Japanese Journal of Biomechanics in Sports and Exercise***, 15(4): 155-161, 2011.

7. Patent

[1] 入來篤史、牛場潤一、武見充晃. 閾値推定装置、閾値推定方法、ならびに、プログラム. 特願2014-229524.